*pmd*CRC*

# Project C1 (Curnamona) Final Report


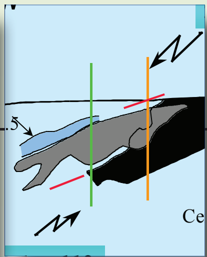

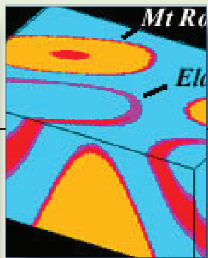


R Anczkiewicz, J Parr, G Carr, R Weinberg, T Lees

pmd*CRC

# *pmd**CRC Project C1

# FINAL REPORT

## Table of Contents

# Lu-Hf isotopes applied to Broken Hill: early metamorphism

**Robert Anczkiewicz**
**School of Geosciences, Monash University**

**Summary**

The timing of initiation of high-grade metamorphism in the Broken Hill Block of the Curnamona Province is a much discussed and essentially missing piece of knowledge related to the tectonothermal evolution of the area. Cooling ages of ca. 1600 Ma from peak metamorphic conditions have been determined using Sm-Nd isotope systematics in garnets, and U-Pb dating of zircons in syn-tectonic and post-tectonic magmatic rocks, and monazites in metamorphic rocks. In this project, six garnet-bearing samples from a variety of rock types from the Broken Hill Block were chosen in an attempt to date the prograde path of metamorphism by means of Lu-Hf isotopes. A methodology was developed to suit the specific samples and analytical conditions available. The isochrons derived for four samples were less than ideal. A single large garnet grain from sample 04-1 from Round Hill, however, produced two reliable isochrons, yielding a growth age of 1635 ± 7 Ma (MSWD=1.1) for the core of the garnet, and 1621 ± 8 Ma (MSWD=1.4) for the rim of the garnet. This suggests the high-grade metamorphism, as dated by garnet growth, started soon after deposition of the Paragon Group at ca. 1640 Ma, and lasted for at least 15 m.y. Growth of garnet rims at ca.1620 Ma coincide with garnet growth inferred from monazite inclusions in garnets from another sample from Round Hill by Forbes et al. (2007). This suggests that the tectonometamorphic event corresponding to the Olarian Orogeny lasted at least 35 m.y., from its inception soon after the end of recorded sedimentation to its cooling at ca. 1600 Ma.

## Introduction

The main objective of the proposed research was to establish the timing of the earliest metamorphic event in the Broken Hill Block of the Curnamona Province. High temperature, migmatitic conditions preserved in most of the study area requires the application of geochronometer(s) with high isotopic closure temperature, which, at the same time, would enable linking isotopic age to the petrological record. The method of choice was Lu-Hf garnet dating. Garnets belong to the earliest metamorphic episode preserved in the Broken Hill area and although major element distribution patterns point to a clearly diffusional origin, heavy REE element analyses conducted by LA ICPMS show bell shape (Rayleigh type) patterns (Fig. 1), which are typically interpreted to represent original growth conditions.

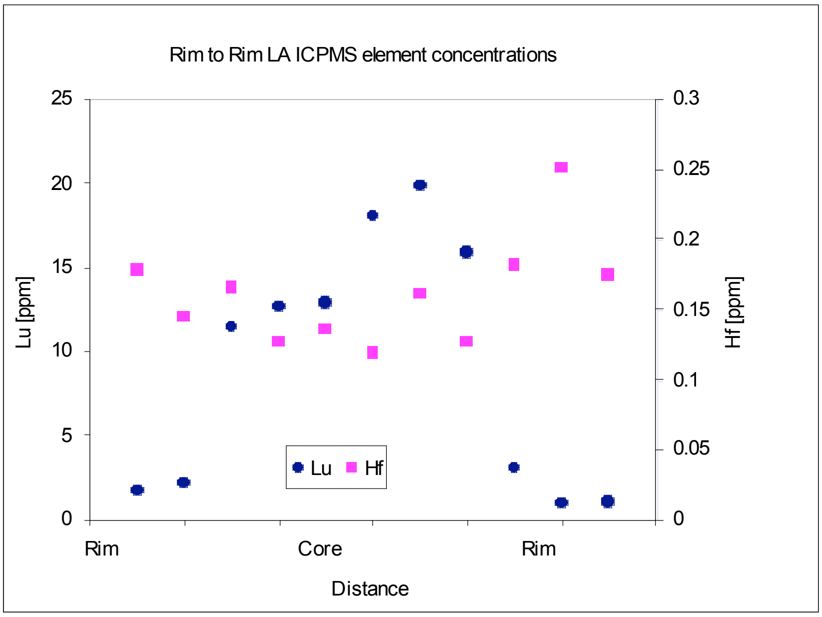


*Figure 1. Typical distribution of Lu and Hf in garnets from metapelites. Garnet from sample 04-1, southern slope of Round Hill.*

Moreover, these patterns reflect rather simple single growth stage. Hafnium zonation trends are typical of the behaviour of incompatible elements, which is reflected in rising concentration from core towards the rim. Any small inversion of this trend (drop in Hf and rise in Lu concentrations) is most likely caused by resorption (Yang and Rivers 2002).

The major obstacle in applying Lu-Hf dating method to garnets in Broken Hill was caused by the presence of a very large amount of zircon inclusions. Zircon being a major Hf carrier in the rocks and containing up to hundreds of thousands times more Hf than garnet, often spoils the Lu-Hf dating. Inherited Hf components, when included in garnets, shift isotopic ratios towards lower values and thus make isochron ages "too young" (providing the initial ratio is accurate). Inherited Hf may also influence the initial ratio determination, if the difference between an episode being dated and inherited component is considerable (Prince et al., 2000; Scherer et al., 2000). Therefore, it was proposed to develop a novel approach to mineral separation and apply leaching techniques, which would considerably diminish the influence of zircons on Hf budget in the analysed samples. Moreover, all fractions were dissolved on a hot plate in order to limit zircon dissolution. Zircon, being strongly refractory mineral, dissolves easily only in pressurised bombs., When metamict, however, zircons are still expected to dominate the Lu-Hf budget.

**Methodology**

The oldest ages interpreted as representing the earliest metamorphic episode in the Broken Hill Block were documented by U-Pb zircon dating of mafic amphibolites and retrogressed mafic granulites (Gibson and Nutman, 2004), who postulated that the onset of HT/LP metamorphism occurred at around 1690-1700 Ma.. Hence, these type of rocks could potentially contain a record of the earliest metamorphic episode in the Broken Hill Block. Garnet dating of the same type of lithologies aimed at verifying zircon ages, whose interpretation in terms of metamorphism is more ambiguous than the interpretation of garnet ages. Migmatitic metapelites are a typical lithology of Broken Hill area and, thus, they also were the primary subject of interest. Moreover, due to the presence of very large garnet crystals, separate core and rim dating could be performed, which would enable some idea about duration of metamorphism and rate of prograde garnet growth to be obtained. Hence, these samples were our primary target. Additionally, zircons in mafic amphibolites are less problematic for garnet geochronology. Thus, five samples were selected for analyses: three metapelites representing the main rock type in the area (04-1, 04-2 from Round Hill area, 01-

51A), two amphibolites (03-50, 03-42F) and one sample representing banded iron formation.

During mineral separation, sample 01-51A appears to contain two different garnet generations (distinct colours). Both garnet types have the same major element composition. This was the only sample, which, on the hand specimen scale, showed some indication of more than one generation of garnet growth.

Garnets were first handpicked from the <400 μm fraction in order to obtain matrix-free separates. Subsequently, they were crushed below about 100 μm in order to expose zircon inclusions. Next, a hand magnet was used, which allowed the separation of garnet from large zircon crystals.

During the course of the project, Robert Anczkiewicz fully established Lu-Hf and Sm-Nd chemistry for isotopic analyses at the School of Geosciences, Monash University. In addition, he upgraded the clean laboratory, which was required in order to carry out the proposed research. Crushed garnet fractions were leached in two steps: 1) with concentrated HF in an ultrasonic bath for about 1.5 hours. Subsequently, the sample was centrifuged. The leachate was then separated. In step 2) the residue was further leached with 6M HCl in an ultrasonic bath. Again, the sample was centrifuged. The HCl leachate was joined with the HF leachate and spiked. The residue was spiked and subjected to the full dissolution procedure. Leachates and residues were then analysed separately.

For the purpose of establishing garnet growth rates, and hence the pace of prograde metamorphism, large garnet crystals from the Round Hill area east of the Broken Hill township were selected. Large crystals enabled the mechanical separation of core and rim, which were analysed separately. Three garnet fractions were prepared from the core and rim areas. Only one out of three samples (for core and rim) was subjected to leaching according to the scheme outlined above.

**Results**

The summary of Lu-Hf analyses is presented in Table 1. All analyses were conducted in the Geology Department, Royal Holloway University of London, UK. More detailed description of mass spectrometry procedures and dissolution procedures are presented in Thirlwall and Anczkiewicz (2003) and Anczkiewicz et al. (2003). Over the course of the analyses, the performance of the MC ICPMS IsoProbe was monitored with the JMC 475 Hf standard. The average value of $^{176}Hf/^{177}Hf$ = 0.282182±13 (2 standard deviations error) normalised to $^{179}Hf/^{177}Hf$= 0.7325 was obtained. Age calculations were conducted using Isoplot (Ludwig, 2003) applying the decay constant $\lambda_{176Lu}$= 1.865E-11 (Dalmasso, 1992; Scherer et al., 2003). $^{176}Lu/^{177}Hf$ errors are 0.5%. A mixed $^{176}Lu$-$^{180}Hf$ spike was used. The total analytical blank was below 30 pg, and thus, its contribution to analyses was neglected.

**Sample BIF** shows a limited spread among the analysed garnet and whole rock fractions, which resulted only in a very low quality isochron age of 1550±75 Ma. Rather surprisingly, the whole rock analyses showed little reproducibility, which is likely to result from incomplete dissolution of refractory minerals. The garnet analyses show significant variations too, which is caused by different qualities of the prepared separates. Fraction g2 was of greater purity, while fraction g1 still contained a minor contamination of matrix minerals. An overall high scatter of the individual data points did not allow the obtaining of a precise age.

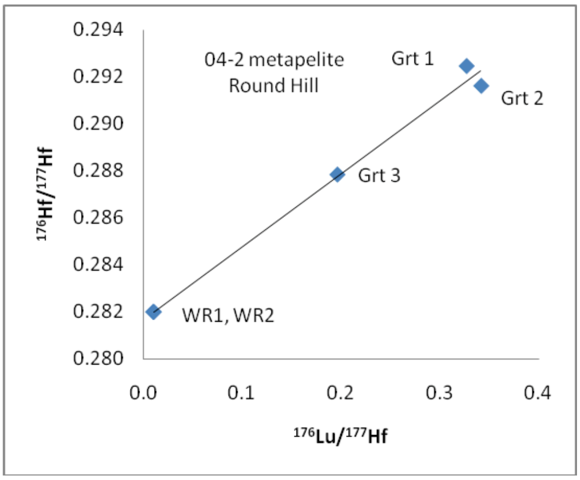


*Figure 2. Isochron diagram for sample 04-2.*

The results obtained for **Sample 04-2** from the Round Hill area are strongly scattered and do not define an age. They point to the overwhelming influence of Hf-rich inclusions, which dominated the Lu-Hf budget in the garnet. Although the isotopic composition of Hf from both whole rock fractions is very well reproduced, the corresponding $^{176}Lu/^{177}Hf$ ratios are outside their analytical error. Also, the obtained concentrations of both elements show strong variation, which is likely to be caused by the spike or sample weighing errors. All three garnet fractions show significantly different isotopic compositions and element concentrations.

*Table 1. Summary of Lu-Hf dating results. Abbreviations: wr- whole rock, g-garnet, f-fraction, L- leachate.*

| | Lu [ppm] | Hf [ppm] | $^{176}Lu/^{177}Hf$ | $^{176}Hf/^{177}Hf$ | Age [Ma] | |
|---|---|---|---|---|---|---|
| BIF (Broken Hill town) | | | | | | |
| wr1 | 0.235 | 2.165 | 0.0154 | 0.282094±8 | | |
| wr2 | 0.249 | 2.351 | 0.0149 | 0.282063±11 | | |
| g1 | 0.568 | 1.276 | 0.0630 | 0.283507±20 | | |
| g2 | 0.571 | 0.838 | 0.0963 | 0.284443±27 | | |
| 42F (54J UTM 522900 mE 6466810 mN) | | | | | | |
| g2 | 0.396 | 1.557 | 0.0359 | 0.282835±11 | | |
| g1 | 0.569 | 2.182 | 0.0369 | 0.282839±19 | | |
| wr | 0.578 | 2.201 | 0.0371 | 0.282834±12 | | |
| 03-50 (54J UTM 552548E and 6452754N) | | | | | | |
| g2 | 4.814 | 1.313 | 0.5201 | 0.297720±11 | | |
| g1 | 3.025 | 0.225 | 1.9205 | 0.340263±19 | | |
| wr | 1.939 | 0.394 | 0.7022 | 0.330674±12 | | |
| 01-51A (54J UTM 548910E and 6467250N) metapelites (sample RHA51 in Forbes et al. 2007) | | | | | | |
| wr | 0.601 | 5.329 | 0.0160 | 0.282222±9 | | |
| g 1 red | 5.587 | 2.210 | 0.3581 | 0.291917±10 | 1500 | |
| g2 orange | 6.246 | 2.073 | 0.4271 | 0.294838±7 | 1621 | |
| 04-1 Round Hill metapelite (54J UTM 548620 mE 6467194 mN) (high resolution dating of single garnet crystal) | | | | | | |
| core res | 56.243 | 8.694 | 0.9193 | 0.309382±20 | | |
| core g.L1 | 24.874 | 12.879 | 0.2735 | 0.290555±25 | | |
| core fA | 60.035 | 18.471 | 0.4608 | 0.295895±37 | 1635±7 | MSWD=1.1 |
| core fB | 56.931 | 17.082 | 0.4725 | 0.296321±29 | | |
| L rim | 19.476 | 17.974 | 0.1534 | 0.286611±30 | | |
| RES rim | 30.217 | 11.521 | 0.3716 | 0.292953±35 | | |
| fD rim | 29.741 | 13.129 | 0.3209 | 0.291486±29 | 1621±8 | MSWD=1.4 |
| fB rim | 33.354 | 16.974 | 0.2783 | 0.290232±30 | | |
| WR1 | 0.646 | 4.411 | 0.0207 | 0.282293±27 | | |
| WR2 | 0.386 | 3.872 | 0.0141 | 0.282109±33 | | |
| 04-2 Round Hill metapelite (54J UTM 548620 mE 6467194 mN) | | | | | | |
| wr1 | 0.512 | 7.404 | 0.0098 | 0.281979±8 | | |
| wr2 | 0.851 | 11.387 | 0.0106 | 0.281976±7 | | |
| g1 | 6.294 | 2.731 | 0.3265 | 0.292450±6 | | |
| g2 | 8.600 | 3.569 | 0.3413 | 0.291605±10 | | |
| g3 | 14.482 | 10.461 | 0.1960 | 0.287827±14 | | |

These differences correlate, to a large degree, with their treatment prior to analysis. Fractions g1 and g2, which yielded higher isotopic ratios, are the most magnetic components, which allowed the avoiding, to some extent, of zircon contamination. Fraction g3 is the least magnetic and is the richest in zircon inclusions. This observation is confirmed by the concentrations of Lu and Hf. Garnets g1 and g2, although purer, still show very high Hf concentrations and are over ten times higher than expected on the basis of the LA ICPMS analyses (Fig. 1). Fraction g3, however, shows Hf concentration almost 100 times higher than expected. This shows that magnetic separation can significantly improve the quality of minerals subjected to Hf analyses. Crushing the garnet fractions to a significantly smaller size than 100 μm almost certainly would bring further improvement, since it leads to release of smaller zircon crystals from the garnet.

All fractions from **Sample 42F** yielded identical isotopic composition within error, which precludes any age constraints (Table 1). Low Lu/Hf ratios observed in this sample are unlikely to be caused by inclusions. It seems more likely that low Lu content in this rock, and in its garnets, is a primary feature.

**Metapelite 01-51A** shows similar characteristic to sample 04-2. For both samples, age determination is impossible due to the high scatter of the individual data points, despite yielding sufficiently high Lu/Hf ratios. Two garnet fractions separated on the basis of their colour correspond to a 1500 Ma age (g1) and a 1621 Ma (g2). Thus, they could reflect different stages of garnet growth. None of the garnet analyses, however, were confirmed with a replicate sample and are thus considered suspect.


*Figure 3. Sample 04-1, Round Hill area. Large garnet crystals used for Lu-Hf analyses.*

A single garnet crystal was analysed from **Sample 04-01,**. Due to the large size of the garnets (Fig. 3), separate core and rim analyses were performed. Two whole rock fractions were analysed to constrain the $^{176}Hf/^{177}Hf$ initial ratio. All fractions show high Hf concentrations, which clearly points to the contribution of zircons to the Hf budget, despite our efforts to remove the effects of the zircon. Lutetium concentrations, however, are still high enough to guarantee a reasonable spread in $^{176}Lu/^{177}Hf$ ratios and enable good age estimates. Two garnet fractions representing the core and two whole rock powders form an isochron yielding a 1635±7 Ma age (Fig. 4a). When leachate and residue data obtained for the third leached garnet core fraction were added to the isochron, its quality becomes significantly worse. The same is observed for the rim fractions. When leachate and residue data are excluded from age calculations, the remaining four points (two garnet rim fractions and the same two whole rocks), again yield a rather good quality date of 1621±8 Ma. This indicates problems with the leached fractions. The most likely reason for this increased scatter of the points in the isochron is an artificially induced Lu/Hf fractionation during leaching. Due to the contrasting chemical properties of these two elements, the HF leaching step can fractionate Lu and Hf. The subsequent step, which consists of HCl leaching and rejoining the leachate, is aimed at eliminating this fractionation problem. Although this method has been demonstrated to be successful, it failed in the present study.

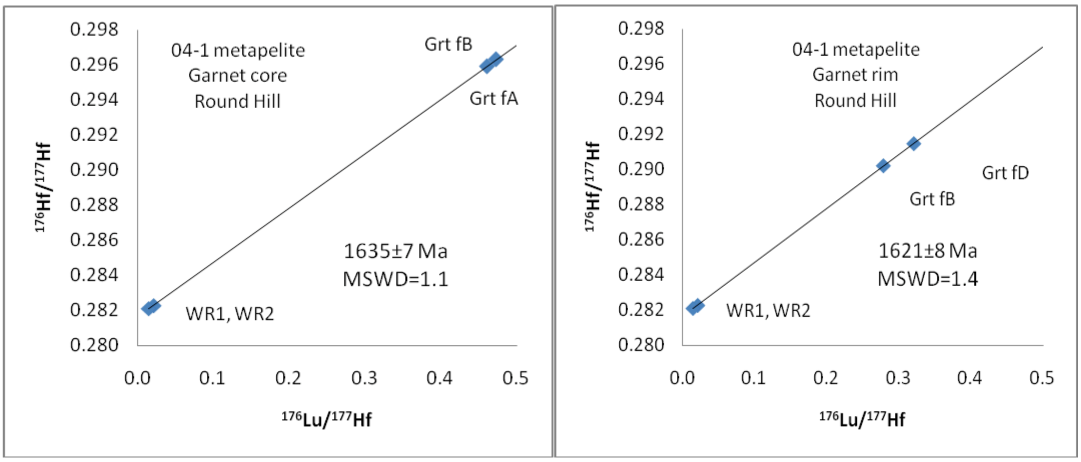


Figure 4. Isochron diagrams for garnet core (left) and garnet rim (right) dating from sample 04-1.

Although the two whole rock fractions for this sample did not yield identical isotopic ratios, they fit well on both isochrons that they form with the garnets (Figs. 4a and 4b). These variations can be attributed to the variable degree of Hf being released primarily from rutile, which is very abundant, and from zircons, during digestion. Inheritance, however, does not seem to be a severe problem in this garnet sample. Typically, mixing of Hf from garnets with Hf from inherited zircons and whole rock should result in high scatter of data points. Yet, garnets and their duplicates, together with whole rocks, form good quality regression lines (MSWD 1.1 and 1.4). Thus, it is concluded that Hf-rich inclusions affected mainly the precision of the results (by lowering parent/daughter ratios) but did not significantly affect their accuracy.

The analysed crystal from sample 04-1 is so large that any post-growth high temperature metamorphism would not significantly affect it. Closure temperature for the Lu-Hf system is not absolutely defined but is expected to be higher than for Sm-Nd, which for such large crystals is in excess of 800 °C (Ganguly et al. 1998). The observed resorption in the rims affects a very small proportion of the analysed rims, and did not contribute significantly to the overall Lu-Hf budget. Thus, our results for sample 04-01 are interpreted as representing prograde garnet growth between 1635 and 1620 Ma, pointing to a 15 m.y. period for garnet growth.

**Concluding remarks**

Lu-Hf dating of metabasalt, which does not suffer from problems with Hf-rich inclusions, unfortunately yielded very low Lu/Hf ratios and did not allow age estimates, due to insufficient variations in Lu/Hf ratios between the garnet and whole rock. In situ trace element zonation profiles, obtained on selected metapelites, display a prograde zonation pattern for Lu and Hf which makes the Lu-Hf geochronometer particularly useful for determining the age of prograde metamorphism. Unfortunately, high concentrations of zircon inclusions caused failure of most attempts to date the garnet growth. Methodological improvements initiated here, with the aim of eliminating or significantly reducing the influence of zircon inclusions in garnets, showed some good prospects, but need further development. A single large garnet grain from sample 04-1 from the Round Hill area yielded the most interesting results. Separate core and rim dating indicate prograde garnet growth occurred over a period of about 15 m.y., between 1635 and 1620 Ma. This is within the range of previously published estimates of growth rates, which vary from about 3 to over 20 m.y. (e.g. Vance and Onions, 1992; Ducea et al., 2003; Kylander-Clark et al., 2007). Our data suggest that prograde metamorphism began at about 1635 Ma, or possibly slightly earlier (taking into account that the core is not represented by a single point but by an average age for the core areas). This estimate is significantly younger than previous estimates of the timing of the early metamorphic event in the Broken Hill Block obtained predominantly by U-Pb SHRIMP technique on zircons from amphibolites and retrogressed mafic granulites (Gibson and Nutman, 2004), which suggested the onset of a high- temperature, low-pressure (HTLP) event between 1690-1670 Ma. The 1635 Ma beginning of HTLP metamorphism determined here correlates much better with estimates obtained from U-Pb zircon and monazite inclusion in garnets, also from Round Hill, yielding garnet growth at around 1620 Ma ages (Forbes et al., 2007; Nutman & Ehlers, 1998). This is the same age as was obtained here by Lu-Hf for the garnet rim of sample 04-1, and for the orange fraction of the Forbes et al. (2007) sample 01-51A from Round Hill. The age for 01-51A, however, must be treated with caution as this it is based on only one garnet fraction.

The 15 m.y. period for garnet growth has some interesting implications for garnet geochronology. Almost all studies presenting garnet dating are based on bulk garnet separates. If individual garnet separates are not well-averaged (i.e., all separates contain the same proportion of core and rim), they will significantly contribute to the scatter of the data points on the isochron diagrams, increasing the MSWD value and largely magnifying errors of the age estimate. On the other hand, well-averaged fractions result in highly precise dates, which take into account potentially the very long growth period for garnet.

**References**


Anczkiewicz, R., Platt, J.P., Thirlwall, M.F. and Wakabayashi, J., 2004. Franciscan subduction off to a slow start: evidence from high-precision Lu-Hf garnet ages on high-grade blocks. Earth Planet. Sci. Lett., 225: 147-161.

Dalmasso, J., Barci-Funel, G. and Ardison, G.J., 1992. Reinvestigation of the decay of the long-lived odd-odd 176Lu nucleus. Applied Rad. Isot., 43: 69-76.

Ducea M.N, Ganguly, J., Rosenberg, E.J., Patchett, P.J., Cheng, W. and Isachsen, C., 2003. Sm-Nd dating of spatially controlled domains of garnet single crystals: a new method of high-temperature thermochronology, Earth Planet. Sci. Lett., 213,31-42.

Forbes, C, Giles, D., Betts, P.G., Weinberg, R. and Kinny, P.D., 2007. Dating prograde amphibolite and granulite facies metamorphism using in situ monazite U-Pb SHRIMP analysis, Jour. Geol., 115, 691–705

Ganguly, J., Tirone, M. and Hervig, R.L., 1988. Diffusion kinetics of samarium and neodymium in garnet, and a method for determining cooling rates of rocks. Science, 281: 805-807.

Gibson, M. and Nutman, A.P., 2004. Detachment faulting and bimodal magmatism in the Palaeoproterozoic Willyama Supergroup, south–central Australia: keys to recognition of a multiply deformed Precambrian metamorphic core complex. J. Geol. Soc. London, 161, 55-66.

Kylander-Clark, A.R.C., Hacker, B.R ., Johnson, C.M., Beard, B.L., N.J., Mahlen, N.J. and Lapen, T.J., 2007. Coupled Lu–Hf and Sm–Nd geochronology constrains prograde and exhumation histories of high- and ultrahigh-pressure eclogites from western Norway. Chemical Geology, 242, 137-154.
Ludwig, K.R., 2003. User's Manual for Isoplot 3.00: a geochronological toolkit for Microsoft Excel. Berkeley Geochronology Centre Special Publication 4.
Nutman, A. P. and Ehlers, K., 1998. Evidence for multiple Palaeoproterozoic thermal events and magmatism adjacent to the Broken Hill Pb-Zn-Ag orebody, Australia. Precamb. Res., 90, 203–238
Scherer, E.E., Cameron, K.L. and Blichert-Toft, J., 2000. Lu-Hf garnet geochronology: Closure temperature relative to the Sm-Nd system and the effects of trace mineral inclusions. Geochim. Cosmochim. Acta, 64(19), 3413-3432.
Scherer, E.E., Munker, C. and Mezger, K., 2001. Calibration of the lutetium-hafnium clock. Science, 293, 683-687.
Thirlwall, M.F. and Anczkiewicz, R., 2004. Multidynamic isotope ratio analysis using MC-ICP-MS and the causes of secular drift in Hf, Nd and Pb isotope ratios. Int. J. Mass. Spect., 235(1), 59-81.
Vance D. and O'Nions R. K. 1992. Prograde and retrograde thermal histories from the Central Swiss Alps. Earth Planet. Sci. Lett., 114**,** 113–129
Yang, P. and Rivers, T., 2002. The origin of Mn and Y annuli in garnet and the thermal dependence of P in garnet and Y in apatite in calc-pelite and pelite, Gagnon terrane, western Labrador. Geol. Res. Materials, 4(1), 1-35.

# Hydrothermal History of the Curnamona Terrain
# Assessment of Pb Isotope and
# Metallogenic Associations

**J.M. Parr and G.R. Carr**
**CSIRO Division of Exploration and Mining**

## Introduction

This report covers work undertaken in the Curnamona Pb isotope project.

## Milestones Achieved

- Acquisition and entry of data and information relating to existing Pb isotope analyses for the Curnamona Province
- Sampling of galena-bearing rocks and other selected ore-related rocks for petrographic and isotopic analysis
- Analysis of galenas from the Line of Lode and galena-bearing rocks and high Pb rocks from a variety of deposits (collected with Barney Stevens and Richard Barratt) (See Appendix 1: file "Parr & Carr analyses.xls" on accompanying CD)
- Potential source rocks with good chronological control identified using petrographic and geochemical discrimination from Geoscience Australia collection.

## Work Undertaken

*Collation of available data*
All available information for existing analysed samples has been collected and collated. The information is appended as Appendix 2 as an electronic version in the file "Parr & Carr old sample information.xls" (see accompanying CD).
In detail:

- Data from documents associated with the CSIRO database (eg Sirotope reports) have been transferred to a spreadsheet in preparation for incorporation in the Pb isotope program "Pb Graph"
- A hard copy of Rio Tinto's data file was obtained by Tim McConachy and much valuable information, particularly AMG coordinates of samples has been transferred to the same spreadsheet
- Information, including old reports and samples, from the old CSIRO Broken Hill mineral collection – the "AB Edwards collection" has been examined and any relevant information noted. These samples may prove to be a useful source of now inaccessible orebodies.

*New Samples*

Four days were spent in the field with Barney Stevens. Emphasis was on collecting samples from a variety of deposit types and stratigraphic positions. Galena-bearing rocks and/or rocks containing plumbian feldspar, were sampled mostly from dumps close to old mine workings where we were confident that they were locally derived and the location was well constrained (i.e. AMG coordinates). On the same field trip, additional information and samples were collected from:

- the Line of Lode and a variety of small BH-type deposits in the vicinity of the mine (from Tony Webster),
- a suite of samples from lenses in the Line of Lode (from Jane Murray), and
- mineralised drill core from the Polygonum Prospect (Mundi Mundi Plain, selected by Richard Barratt (NSWGS) in consultation with, Wolf Leyh (Eaglehawk) which will provide important information about mineralisation in the Paragon Group.

*Summary of samples collected*

- Line of Lode (all located): different orebodies and styles of mineralisation
- BH-type deposits (including the Pinnacles Deposit), Silver King-type (including Silver King)
- Late stage galena-bearing veins ("Thackaringa-type")
- Other: W-bearing ("Corruga-type"), Cu-Au–enriched (e.g. Diamond Jubilee), base metals in qtz-fluorite veins (e.g. Mt Robe), base metals in calc-silicates ("Ettlewood-type").

## Results

The data are presented in file "Parr & Carr analyses.xls" (see accompanying CD) and define three distinct populations[1]:

1. Broken Hill type: data that lie within the Broken Hill ellipse as defined by pre-existing data from the Broken Hill orebody, new data for the Broken Hill orebody and Broken Hill-type occurrences (Figs 1 and 2)
2. A heterogeneous population that have slightly elevated $^{206}Pb/^{204}Pb$ ratios relative to the BH group (Figs 3 and 4) and include the Silver King Mineralisation
3. An even more heterogeneous population with elevated radiogenic Pb (Fig. 5)

### Group 1

*Broken Hill orebody:*

Twenty-nine samples have been analysed in this study from the Line of Lode. The data are all within analytical error of the conventional analytical technique, as can be seen from a comparison with the 95% confidence ellipse in Figure 1. This represents an astounding homogeneity and indicates the ore was formed from a single fluid that showed no isotopic variability over its life and with no later overprinting from a separate fluid, or that the ore was homogenised by melting of galena during granulite facies metamorphism. It is possible that with higher precision double spike or MC-ICPMS data there may be some variation seen – in particular the 1 Lens Dropper sample (14670, Plot Pt 13 in Figure 1; see "Parr & Carr analyses" on accompanying CD).

---

[1] Pb isotope data for Thackaringa-style mineralisation is not discussed here and will be presented in a later report

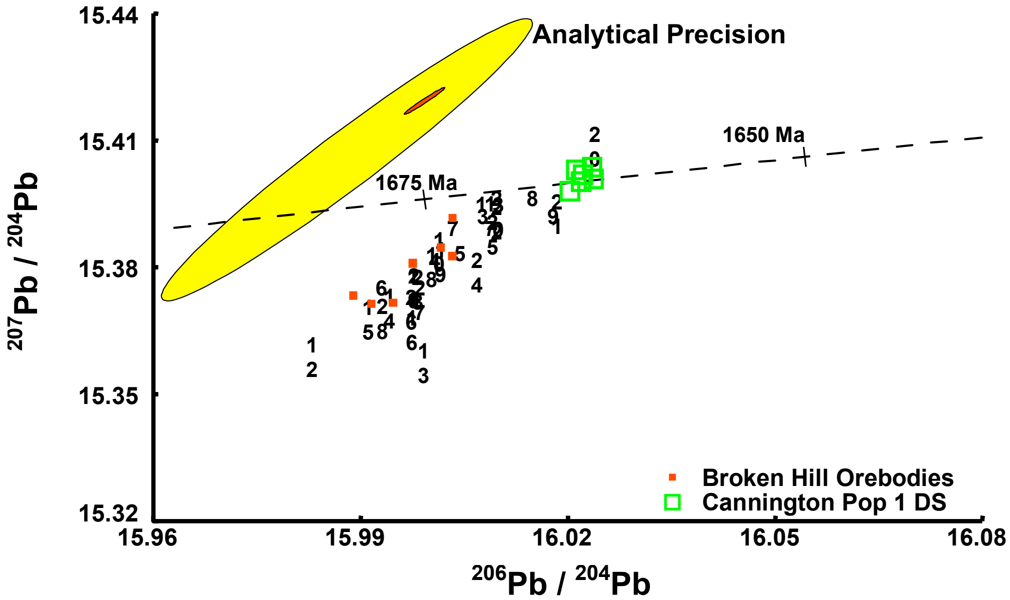


*Figure 1. Conventional Pb isotope diagram comparing results from this study of galena from the Broken Hill orebody, with double spike data from Cannington and the Mount Isa Eastern Fold Belt Growth Curve. This curve was defined based on mineralisation data from the Eastern Fold Belt of Mount Isa and differs from the Western Fold Belt Curve in having lower* $^{207}Pb/^{204}Pb$ *ratios at equivalent* $^{206}Pb/^{204}Pb$ *ratios. The model ages are considered to be accurate to within +/- 10 Ma for the Eastern Fold Belt. At this stage we cannot be confident that these ages are correct for the Broken Hill Terrain. The numbers refer to datapoints in Appendix 3*

*Other Deposits with Broken Hill Signature*

Many other galenas sampled as part of this study have Pb isotopic ratios that fall within the Broken Hill 95% confidence ellipse and thus can be considered to have formed from the same hydrothermal fluid (Figure 2). These samples are from the following locations:

| | |
|---|---|
| *Silver Hill* | *Rising Sun* |
| *Old Silver Peak* | *Champion* |
| *Consolidated Barrier Main Lode* | *Southern Cross (Nine Mile Road)* |
| *Panel 19* | *Nine Mile Mine* |
| *White Leads* | *Sydney Rockwell* |
| *New Silver Peak* | |

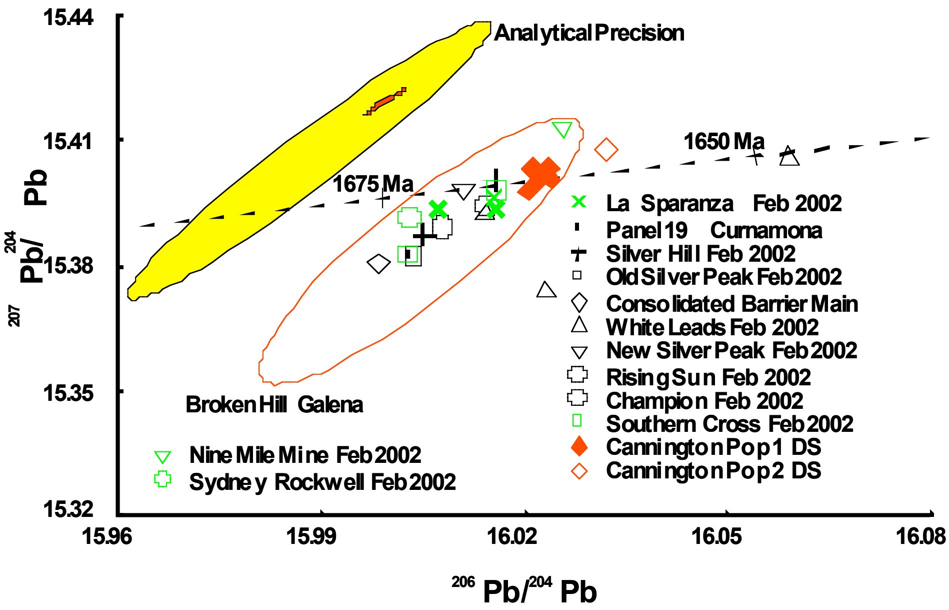


*Figure 2. Conventional Pb isotope diagram showing deposits and prospects with lead isotope ratios indistinguishable from Broken Hill. The data are compared with the Broken Hill 95% confidence ellipse, the 95% confidence ellipse of analytical precision and the Mount Isa Eastern Fold Belt Growth Curve.*

## <u>Group 2</u>

These deposits have Pb isotopic ratios slightly higher than Broken Hill (Figs 3 and 4). In comparison to data at Cannington, in the Eastern Mount Isa Fold Belt, they are similar to the high $^{206}Pb/^{204}Pb$ "tail" which was defined as Population 2 and was associated with paragenetically late galena, probably formed during $D_3$ deformation. These samples are from the following locations:

*SN3*

*Silver King*

*Black Prince*

*Kinchega Rockwell*

*Parnell*

In addition, *White Leads*, has a datapoint within this population as well as in the Broken Hill Signature.

## <u>Group 3</u>

This group is represented by the *Melbourne Rockwell* deposit, which has $^{206}Pb/^{204}Pb$ ratios slightly lower than Broken Hill, indicating a model age approximately 10 Ma older than Broken Hill (Figure 4). These results are similar to those for the Pinnacles deposit.

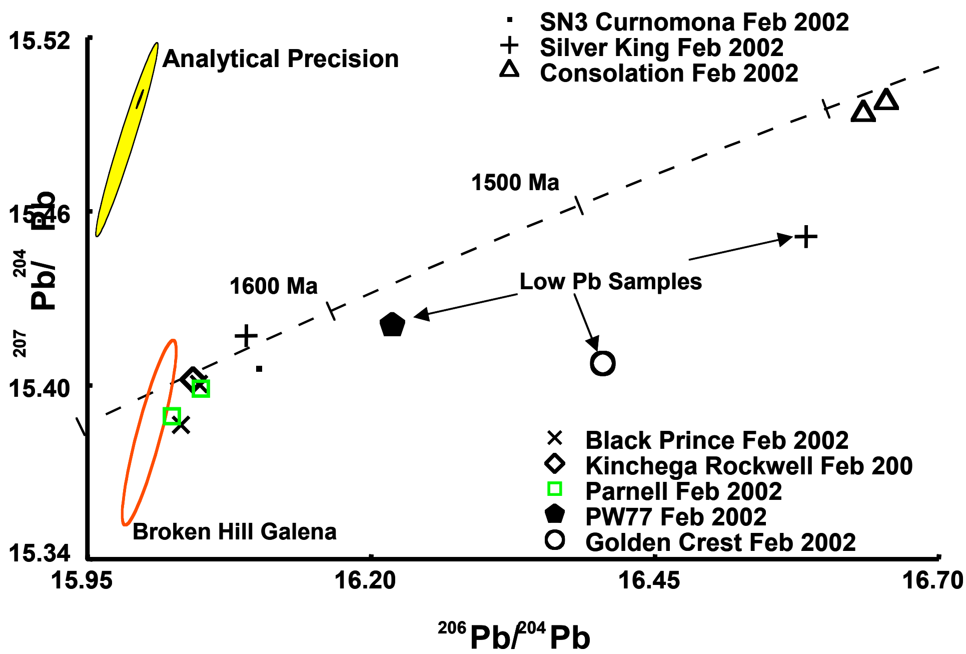


*Figure 3. Conventional Pb isotope diagram showing deposits and prospects with lead isotope ratios slightly higher than Broken Hill. The data are compared with the Broken Hill 95% confidence ellipse, the 95% confidence ellipse of analytical precision and the Mount Isa Eastern Fold Belt Growth Curve*

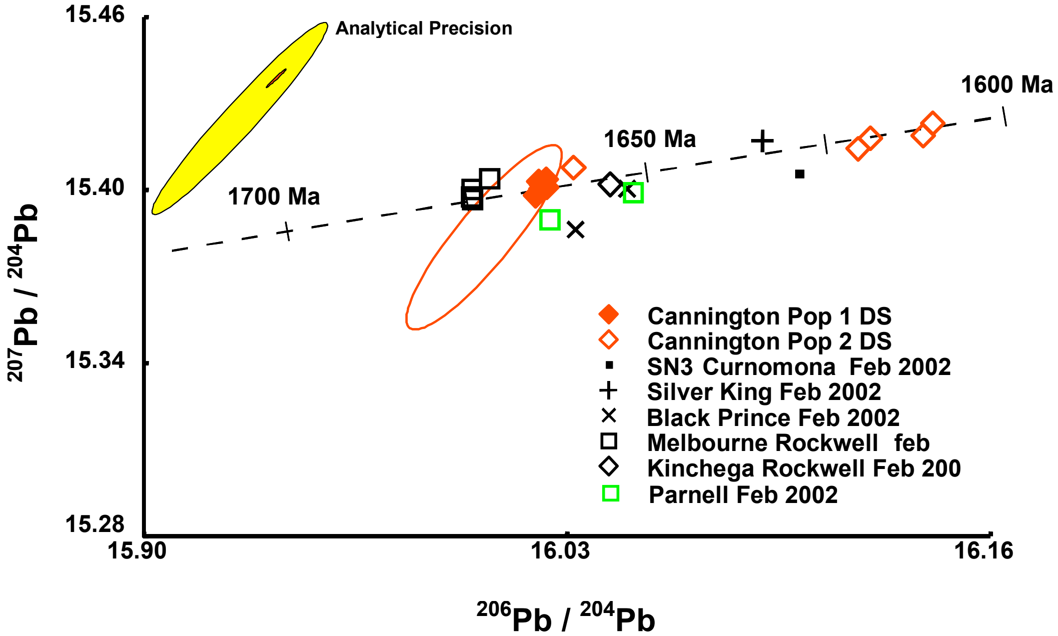


*Figure 4. An expanded scale conventional Pb isotope plot of data from Figure 3. together with data from Melbourne Rockwell, which has $^{206}Pb/^{204}Pb$ ratios lower than Broken Hill. The data are compared with the Broken Hill 95% confidence ellipse, the 95% confidence ellipse of analytical precision and the Mount Isa Eastern Fold Belt Growth Curve and Cannington Population 1 and Population 2 double spike data.*

## Group 4

This data population has very high Pb isotope ratios and probably represents a significantly younger event, or events (Figure 5). It does not appear to be similar to the Thackaringa data (to be discussed in a future report). Deposits in this group are:

| | |
|---|---|
| *SN10* | *Mayflower* |
| *SN54* | *Terrible Dick* |
| *Richard Ruby* | |

## Other data

Results of low-Pb samples from *PW77* and *Golden Crest* are difficult to interpret at this stage (Figure 3). Samples from *Mt Robe* are not consistent with existing Thackaringa mineralisation (Figure 5).

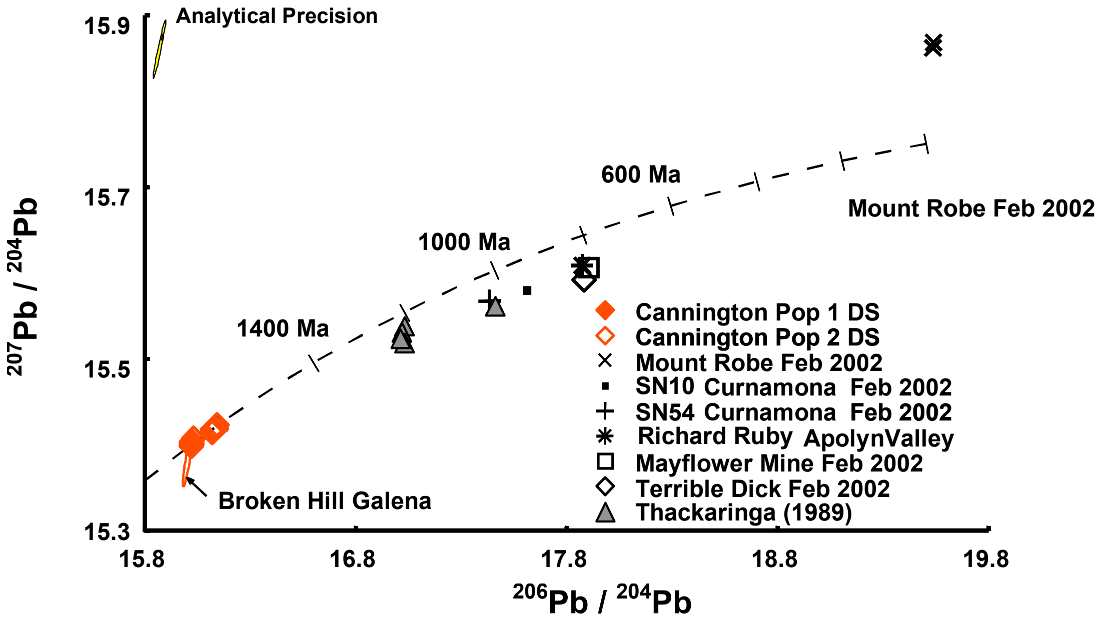


*Figure 5 Conventional Pb isotope diagram showing deposits and prospects with lead isotope ratios significantly higher than Broken Hill. The data are compared with the Broken Hill 95% confidence ellipse, the 95% confidence ellipse form analytical precision and the Mount Isa eastern Fold Belt Growth Curve, Thackaringa Vein data (from 1989) and Cannington data.*

## Preliminary Interpretation

- The main Broken Hill hydrothermal event is well represented in Broken Hill-type deposits distal from the main orebody.
- Younger events are also apparent in the region and are represented by a wide range in $^{206}Pb/^{204}Pb$ ratios suggesting a complex geochronology, perhaps with discrete events intermittent over up to 300 Ma.
- A possible event 10Ma older than Broken Hill is represented by the Melbourne Rockwell data.

**Acknowledgement**

We acknowledge Rio Tinto Exploration (Tim Munday and Ian Ledlie) for providing a hard copy of its Pb isotope computations in the Broken Hill area.

**List of Appendices**

| | |
|---|---|
| Appendix 1: | Pb isotope data ("Parr & Carr analyses.xls" - see accompanying CD) |
| Appendix 2: | Collated information on previous Pb isotope samples. Presented in "Parr & Carr old sample information.xls" (electronic version only - see accompanying CD). |

# Elliptical Structures in W Broken Hill Block: Large Scale Fold Interference Pattern

**Roberto Weinberg**

**Monash University**

Successful mineral exploration needs to be able to predict accurately the continuation at depth of a known mineralisation or of a prospective horizon. For such a job good 3D geological models are required and structural tools have been used for 3D prediction. However, our ability to accurately predict the geometry of complex, poly-folded terranes such as Broken Hill has been relatively limited. This is because prediction requires a detailed lithological map integrated with a detailed structural understanding of the area, and this has historically been missing at Broken Hill.

This report derives the 3D geometry of a poly-folded area in the Broken Hill Block through integrating detailed mesoscale geological documentation of a small area, with the 2D map pattern of rock distribution using *Noddy* and building on previously published ideas (Hobbs et al., 1984). The results explain the complex map patterns while also revealing a likely distribution of lithologies at depth. The method developed here is simple and robust and can be used in other poly-folded terrane. The 3D models can be tested and detailed through inverse modelling of geophysical data such as Airborne Gravity Gradiometry, or TMI.

**Geological Map of the Elliptical Structures, NW Broken Hill Block**

The geological map of the W Broken Hill Block (W of the Apollyon Fault) shows three elliptical structures between 3.5 and 8 km in length defined by the distribution of lithologies. The Eldee structure, close to the Mundi Mundi Fault (Hills et al., 2001, Hobbs et al., 1984) is a ~3.5 x 2 km elliptical ring defined by a ~500 m wide layer containing abundant amphibolite and pegmatite within a partially molten schist, interpreted by the Geological Survey of New South Wales to represent part of the Broken Hill Group. This ring is surrounded by younger Sundown Group rocks, but also enclosed Sundown rocks in its interior. The ring of Broken Hill Group rocks is clearly defined by the red tones in the gamma-ray spectroscopy image shown below, while the Sundown Group rocks inside and outside the ring is well-characterised by the whiteish tones in the same image.

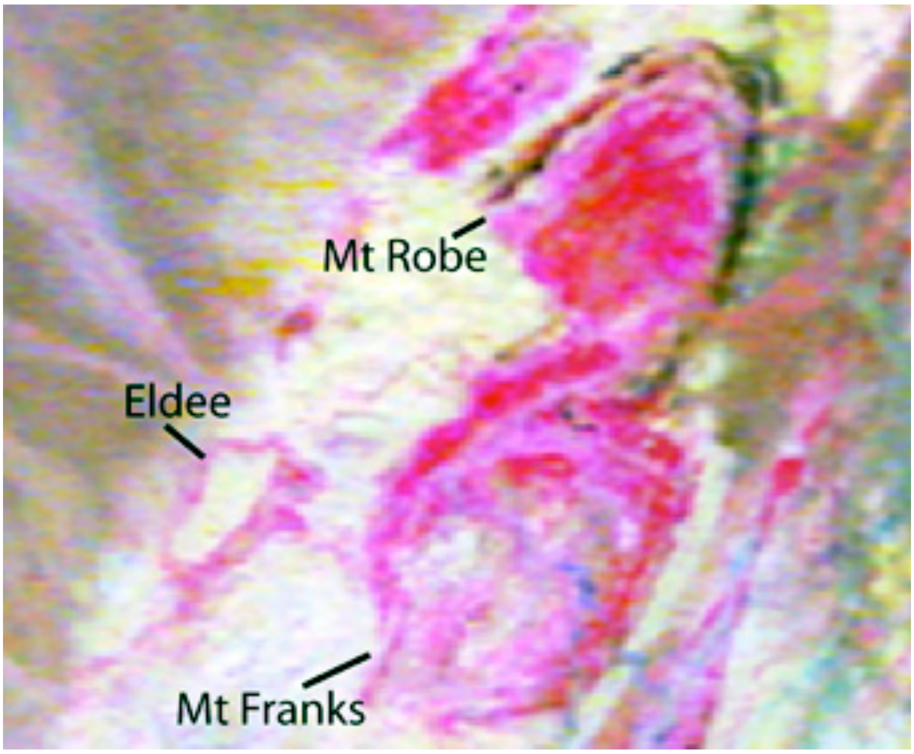


*From BHEI2000 Curnamona Province GIS, AGSO*

The Mt Franks and Mt Robe elliptical structures are larger and different than the Eldee structure. The Mt Robe structure has the Broken Hill Group ring surrounding a core of older Thackaringa Group rocks, rather than the younger Sundown rocks. The Mt Franks structure, by contrast, has Thackaringa Group rocks as part of the ring which surrounds a core of younger Sundown rocks. These three elliptical structures, similar in general but different in their detail, suggest that they resulted from a similar but complex pattern of folding. Hobbs et al. (1984) interpreted these structures as resulting from kilometre-scale interference between upright, N- to NNW-trending folds and NE-trending folds, superimposed on the lower limb of an earlier macroscopic recumbent fold, forming a doubly plunging synformal anticline.

In this study we will show that, in its most simple form, Hobbs et al.'s interpretation explains only the elliptical shape of the structures but not the distribution of rock packages. We build a 3D geometrical model using *Noddy* based on our detailed structural geology work in the area around the Eldee Creek, in the northern margin of the Eldee structure. We show that by modifying Hobbs et al.'s model slightly, the full complexity of the mapped geological pattern emerges. This work provides a 3D geometry which explains the map pattern and can be further tested and refined using geophysical tools.

In this report we first provide a brief and as yet incomplete description of structures mapped around the Eldee Creek. This is followed by a section where the 3D *Noddy* model is built based on our structural understanding. A problem with the relative position between Mt Robe and Mt Franks structures is explored, by inverting the vergence of F2 folds from north to south. This is followed by a study of the possibility that the structures are derived from an early sheath folding event, overprinted by smaller, later folds with no major effect on the broad shape of the structure, and then by "Discussion and Conclusions"

**Mesoscopic Structural Geology**

In this section we briefly demonstrate the interference between fold phases as recorded by rocks around the Eldee Creek in the northern end of the Eldee Structure.

An early deformation phase folds a pre-existing S1//S0 foliation giving rise to inclined to recumbent F2 folds and S2 axial planar foliation (Figs 1, 2 and 3). F2 folds commonly ride a melt-filled detachment thrust plane (Figs 1, 2 and 3).

F2 folds are generally asymmetric and generally verge towards the NE quadrant (anywhere from ~NNW to ~ESE). The variation in their vergence and axial plane orientation is related to refolding by later folds (Fig. 5), and the pattern was interpreted to indicate original vergence roughly to the north, as originally interpreted by Hobbs et al. (1984).

F2 folds are overprinted by an upright, NE-trending S3 foliation and associated folds, that vary from open to tight (Figs 2 and 3). These folds are in turn overprinted by E-W trending S4 foliation and broad folds.

Pegmatites can be found parallel to S0//S1 and folded around F2. They can also be found parallel to the axial planar foliation of F2 folds and associated thrusts (Figs 2 and 3), as well as parallel S3 axial planar foliation (Fig. 4).

*Figure 1. F2 fold riding a melt-filled detachment thrust.*

*Figure 2a. Tight, inclined, asymmetric, N-verging F2 fold developing into a thrust, and refolded by a NE-trending upright F3 fold, top left-hand corner.*

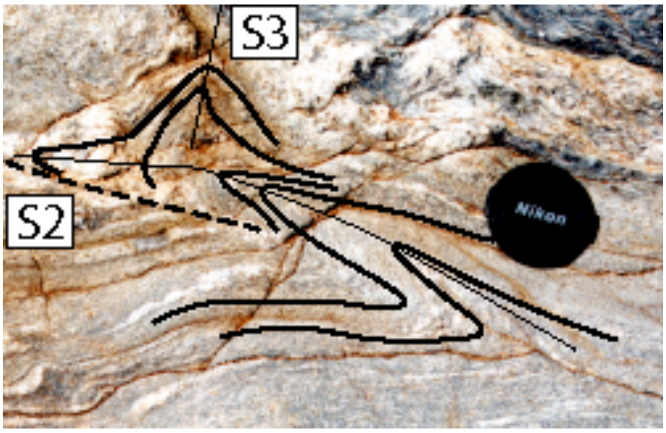


*Figure 2b. Interpretation of Fig. 2a.*

*Figure 3a. Similar to Fig. 2. F2 asymmetric fold and thrust, verging N, cut by a later NE-trending aplitic vein, parallel to S3.*

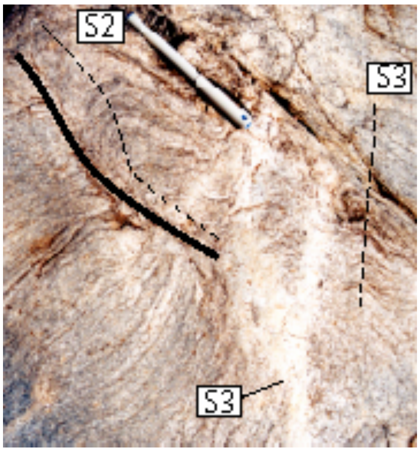


*Figure 3b. Line drawing of Fig. 3a.*

*Figure 4. Pegmatitic veins parallel to S3, cross cutting S1//S0. which also define broad F3 folds.*

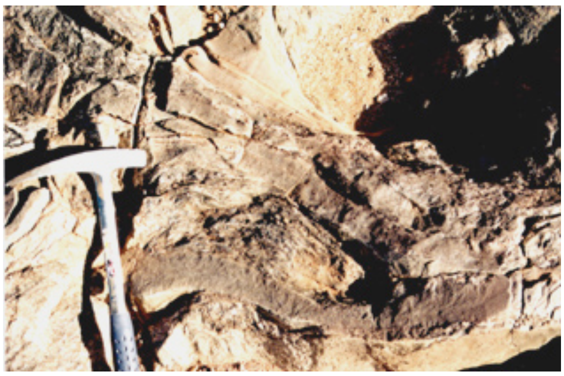

*Figure 5a. F2 folded refolded by F3.*

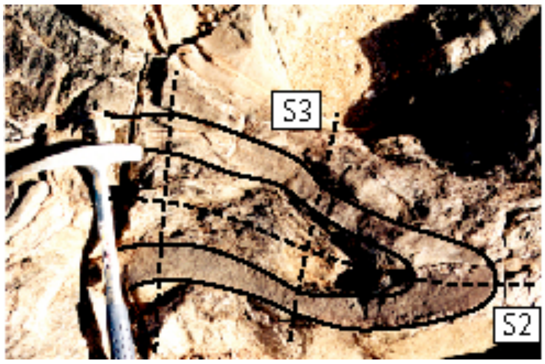


*Figure 5b. Line drawing of Fig. 5a*

*Fig. 6. Summarising figure of the structures*

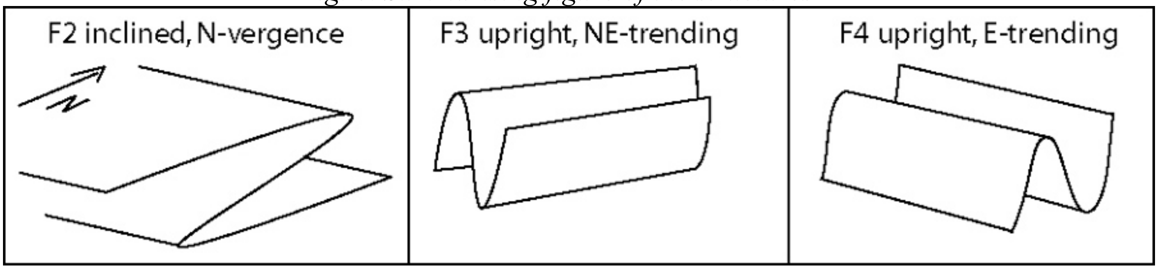


**3D *Noddy* Model**

A 3D model was built using *Noddy* through a few iterations, where the wavelength of all folds was kept constant at 4km, and the amplitudes were varied in order to find best match with the large scale elliptical structures mapped by the Survey. Two models are presented. They are essentially similar except for different thicknesses of the sedimentary package. The absolute value of the sedimentary package is unimportant, the important value is the ratio between fold amplitude/wavelength and package thickness. The three rock Groups that crop out in the elliptical structures are used in the models.

According to Stevens et al. (1983, Records of the Geological Survey of New South Wales) the stratigraphic layers generally have the following thicknesses:

· Sundown Group: from a few hundred meters to 1500m

· Broken Hill Group:~300m to >2000m, approximately 2000m

· Thackaringa Group:<1000m to >3000m, approximately 1500m

MODEL SPECIFICATIONS

| Stratigraphy | Model 1: 7km+ package | Model 2: 3km+ package |
|---|---|---|
| Sundown Group (light blue) | 3 km + | 1 km + |
| Broken Hill Group (red and pink) | 2.5 km | 1 km |
| Thackaringa Group (orange) | 1.5 km+ | 1 km + |

Fold wavelength (all fold phases): 4 km

· Amplitude: variable (see figures below)

Fold Phase

· F2 inclined fold, verging N

· F3 upright fold, trending NE

· F4 upright fold, trending E

**Hobbs et al.'s Model**

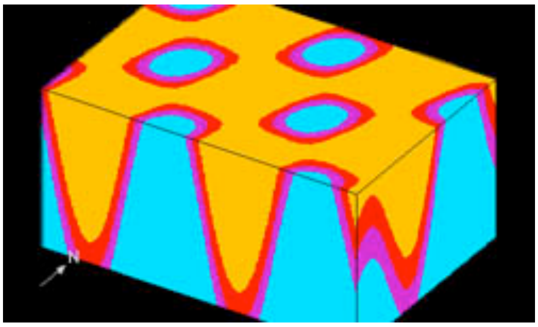

Fig. 7. We start this investigation by testing the 3D model proposed by Hobbs et al. (1984). The model uses an inverted stratigraphy and a NNW-trending upright fold (wavelength 4km, amplitude 2km) overprinted by a NNE-trending upright fold of similar dimensions. The model takes a simple inverted stratigraphy to produce the dome-and-basin interference pattern. The model does not produce the full complexity of the patterns observed in the structures. We will investigate below models that use our structural work, but that are ultimately similar to that of Hobbs et al. but with one small but essential difference: to produce the complexity of the structures, rather than folding an inverted limb of an early fold, both limbs of this early fold need to be folded together.

**New Models**

<u>Model 1. Thick, 7km-package</u>

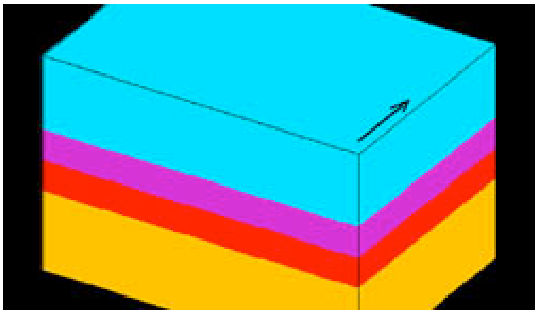

Fig. 8a. Model 1, flat stratigraphic sequence, arrow points to N. S0//S1. The width and length of the top surface are both 10km, and the box is 7km deep.

<u>Model 2. Thin, 3km-package</u>

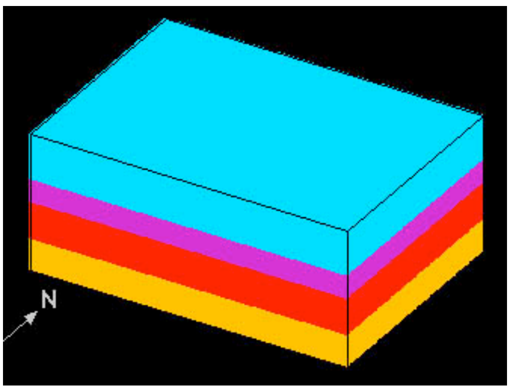


Fig. 8b. Model 2, flat stratigraphic sequence. The differences to Model 1 are the dimensions of the box and the amplitude of the folds. The width and length of the top surface are 7 and 5km respectively, and the box is 3km deep. The dimensions of F2 is the same as in Model 1, but F3-F4 have an amplitude of 2km.

Model 1. F2

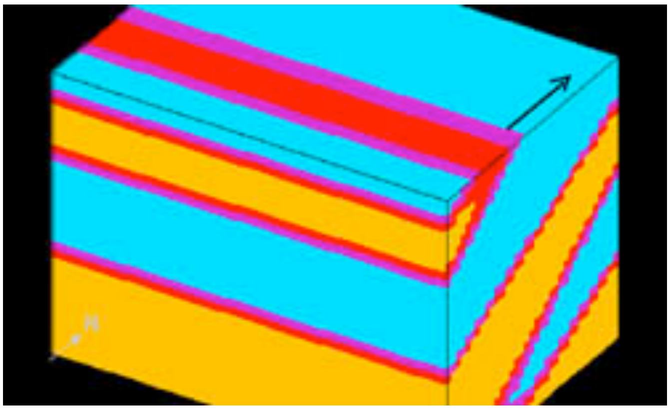

Fig. 9a. F2: inclined 20$^{o}$, N-verging folds, amplitude=8km.

Model 2. F2

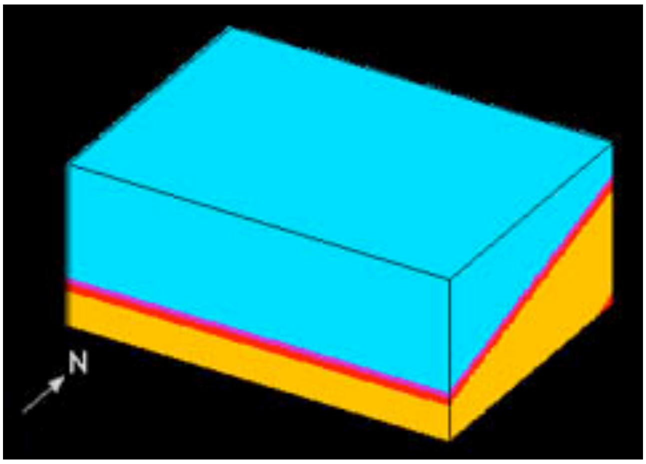


Fig. 9b. Identical fold parameters to those of Fig 9a.

Model 1. F3

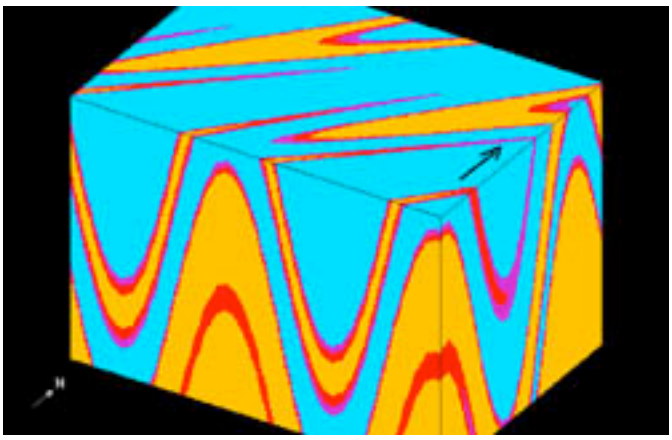

Fig. 10a. F3: NE-trending, upright folds, amplitude=2km. The superposition of these two phases give rise to an interference pattern intermediate between Ramsay and Hubber's Type 2 (mushroom pattern) and Type 3 (convergent-divergent pattern).

Model 2. F3

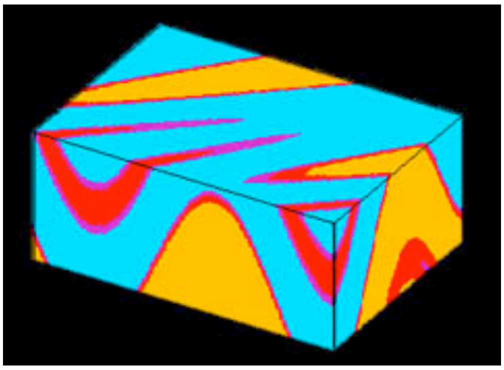

Fig. 10b. Identical fold parameters to Fig. 10a. The difference that controls the patterns is the thickness of the sedimentary package.

Model 1. F4


Fig. 11a. F4: E-trending, upright folds, amplitude=1.5km. Change in the amplitude of F4 up to 4km does not change the shape of the circular structures in their essence. The superposition of the three fold phases documented at mesoscale, give rise to the oval structures observed in the NW part of the Broken Hill Block. In this case, the structure is similar to Eldee, with the youngest Sundown Group rocks both inside and outside the structure separated by a ring of the older Broken Hill Group.

Model 2. F4

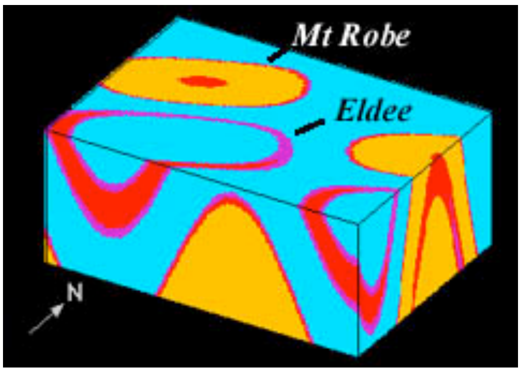


Fig. 11b. Like Fig. 11a but amplitude=2km. Note that this case gives rise to a structure similar to Eldee, and to a structure similar to both Mount Robe and Mount Franks with the older Thackaringa Group rocks forming part of the ring but younger rocks cropping out towards the core. In this case, deeper erosion would expose Sundown Group rocks in the core of the ellipses like documented at Mt Franks.

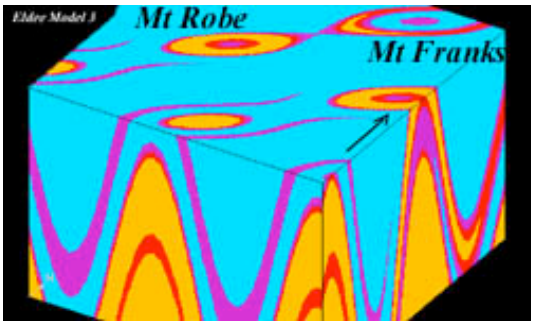


Fig. 12. Same as Fig. 11a, but F4 was superimposed on F3 folds of 4km (instead of 2km) Increasing the amplitude of F2 folds, changes the rock distribution at the surface of the model so that the oval structure has a broadly similar rock distribution to the Mt Robe and Mt Franks structures.

**The Mt Robe-Mt Frank Problem**

In the models above the Mt Robe and Mt Franks structures are relatively well reproduced by the models. However, their relative geographical positions are inverted. The structure most similar to Mt Robe in the models is south of the structure most similar to Mt Franks. The opposite is true in the nature. This is easily fixed by inverting F2 vergence from north to south, as shown in the model below. In this model, the wavelength of F3 folds was changed from 4 to 6km leading to wider ellipsis, and leading also to the two structures being slightly stepped along their length (en-echelon). Furthermore, the amplitude of F4 was modified from 1.5km to 1.3km, in order to slightly enhance the opened shape of the southern Mt Franks structure. In this case the ring is open so that the Sundown Group rocks (in blue) in the core merge with that outside through a gap in the ring on the south side of the structure, similar to the natural analogue.

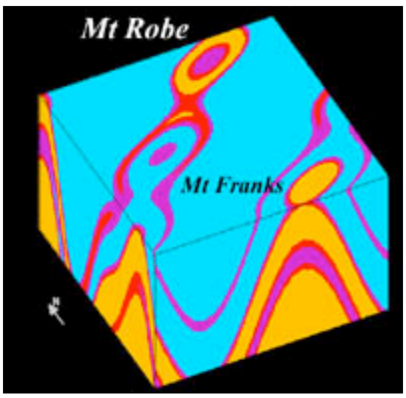


Fig. 13. Interference pattern where F2 verges south, producing Mt Robe and Mt Franks structures in their correct geographic position, including the slight en-ecehlon relationship and the southward merging of core Sundown with external Sundown rocks.

**...and for completion: the "sheath fold model"**

The model put forward by Hills et al. (2000) based on detailed structural work is that the Eldee structure is a result of an early phase (F2) of sheath folds, later overprinted by small scale F3 and F4 folds. Here we test whether an early phase of sheath folds overprinted by F3 and F4 could produce the elliptical structures. Obviously a single phase of sheath folding cannot produce a structure like Eldee with Sundown Group rocks both inside and outside, and we demonstrate further that superimposing another fold phase to a large scale sheath fold does not produce the structures either. We argue that to produce the elliptical structures requires first that the original package be folded in an inclined or recumbent manner, and that this be followed either by a single steep sheath fold phase (not tried here) or by two separate fold phases that produce a dome and basin structure, which is the model we developed above.

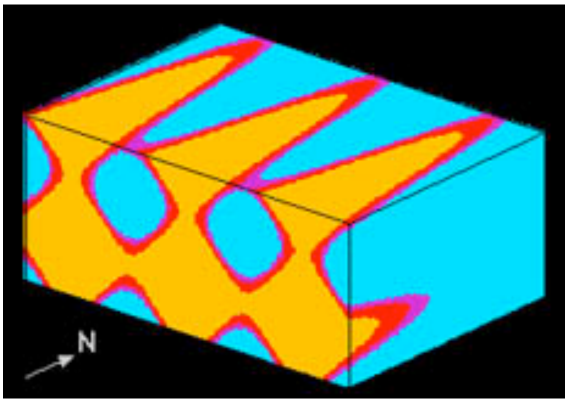


Fig. 14a. Plain recumbent sheath folds formed by a single non-cylindrical fold phase. This model uses the thin sedimentary package, and a wavelength and amplitude of 2.5km.

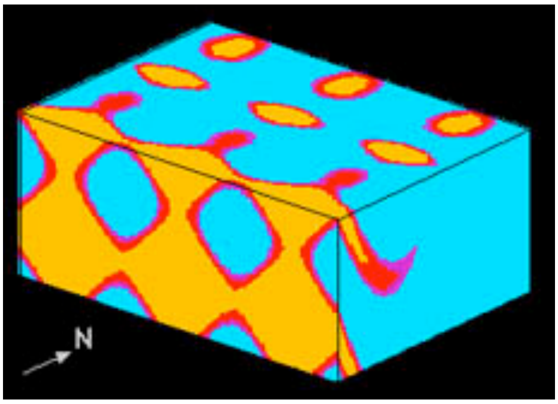


Fig. 14b. Sheath fold in (a) overprinted by an E-W trending upright horizontal fold phase with a wavelength of 6km and an amplitude of 2km. Many variations on the theme were tried including steep sheath folds, and many models, like the one shown above, produces elliptical map patterns but do not reproduce the rock distribution patterns mapped out in Eldee, Mt Robes, Mt Frank.

## Discussion and Conclusions

The Noddy models assume that all three deformation phases developed folds that were expressed regionally at a similar wavelength and amplitudes of the order of kilometres, with an amplitude to wavelength ratios between 0.3 and 2, and wavelength to layer thickness ration of the order of 2.5.

1. Predicting 3D geometry from surface maps is nigh on impossible in the absence of detailed structural knowledge. The distribution of lithologies in 3D cannot be predicted from their surface distribution alone.
2. Three phases of cylindrical folds are required to produce the oval structures which characterise the NW part of the Broken Hill Block. The structures produced by Noddy replicate the map patterns at Eldee, Mount Robe and Mount Franks structures.
3. This work delineates the basic steps necessary to understand the complex 3D geometry of poly-folded rock packages: a) detailed lithological mapping, b) detailed structural analysis, c) integration of the two studies with the help of 3D visualisation tools such as Noddy.
4. The next step in further constraining the 3D geometry of such a terrane is to use the 3D models generate to forward model the geophysical signature of the model and compare to available geophysical surveys. In the case of the Broken Hill Block, gravity studies are the most promising for this purpose, but improved knowledge of densities of rock packages are required.
5. Hills et al. (2001) determined that the N and S closures of the Eldee structure plunges moderately SW and these are linked by limbs dipping to the W defining a slightly flattened W-plunging cylinder. This contrasts to the vertical plunge in our model. This can easily be modified by either tilting the geology to the NE after all folding events or by tilting the axial plane of each folding event.
6. The elliptical structures in surface are approximately 4km long and 1.5km wide. The length and aspect ratio of the structures can be changed by modifying the wavelength of the fold phases. For example by increasing the wavelength of F4 folds from 4 to 6km, the length of the structures increase to 6.5km while the width remains constant. In contrast, if F3 wavelength is increased from 4 to 6km (keeping F4 at 4km), the width of the structures increase to 2.3 km while the length remains close to 4km (Fig. 13).

7. Using north-vergence for F2 folds results in the Mt Robe structure being south of the Mt Franks structures, opposite to what has been mapped. This is solved by inverting the vergence of F2 folds, in contradiction to our inference based on field work in the Eldee Creek area. This could be a result of our information on vergence being derived from a single limb of a large scale fold. More work needs to be done to establish this.

8. *This work uses tools that did not exist at the time the seminal work of Hobbs et al. (1984) was produced. Using Noddy we were able to fine tune the conceptual understanding that they developed two decades ago.*

**References**

BHEI 2000 Curnamona Province GIS, AGSO.

Hills, Q.C., Giles, D., Rosenbaum, G., Forbes, C., Lister, G.S., 2001. The Eldee structure: a kilometre-scale sheath fold at the northwestern margin of the Broken Hill Block, NSW, Australia; SGTSG Abstracts, Ulverstone, Tasmania, 64, p. 81-82.

Hobbs, B.E., Archibald, N.J., Etheridge, M.A., Wall, V.J., 1984. Tectonic history of the Broken Hill Block, Australia; *in* Kroner and Greiling, (eds) Precambrian Tectonics Illustrated, p. 353-368.

# A metasomatic model for Broken Hill: a hypothesis

**Terry Lees**

**School of Earth Sciences, University of Melbourne**

**Summary**

The hypothesis presented is that many of the features of the Broken Hill deposit were produced by metasomatism of a pre-existing sulphide deposit. Using Broken Hill as an example of the enigmatic class of Broken Hill-type deposits, features of the class (alteration styles, ore grade and mineralogy) are explained.

The process envisaged is that a pre-existing Zn, Pb bearing sulphide was partially dissolved by metamorphic dehydration fluids to form a hot metasomatic metal-bearing fluid. Presence of this fluid then triggered local partial melting with generation of abundant pegmatite melt, which in turn reacted with the metal bearing fluid to form quartz-gahnite, lode pegmatite and release silica and potassium. Abundant silica was available to form the extensive siliceous (-garnet) alteration, as well as silicate in the gangue.

Fractionation of a hot, dense and sinking metal-bearing fluid causes deposition of stacked, saddle reef-like lenses becoming progressively richer in grade and Ag:Pb:Zn ratios downwards. Zone refining is a process invoked to explain the systematic upgrading of ore lenses during deposition of these from the metasomatic fluid. Ore deposition is synchronous with shearing, with a well-defined structural zone, the "Main Drag Fold" which is a dilational position within a high-grade shear zone. Thin garnetite rims were formed around the most evolved ores (2 and 3 lenses) during the late stages of the prograde event and again during the retrograde event around "droppers".

As many of the BHT features (ore mineralogy and grade; alteration) explained by this model as being metasomatic, it can be conjectured that the pre-existing sulphide system may have been similar to sediment-hosted massive sulphide deposits such as Century and Dugald River, containing Zn, Pb, Ag, Mn, Fe and Ca.

## Introduction

The problem of understanding a mineral system has an extra level of complexity in Broken Hill, which is to extract the relevant data about the mineral system through the metamorphic overprint. Lead isotope work indicates the ore was emplaced prior to metamorphism. Many authors have concluded the overprint has simply metamorphosed the deposit *in situ* and isochemically, while Hodgson (1975a, b) argued for a significant degree of metasomatism.

The hypothesis presented is that many of the unique features of Broken Hill including the alteration, ore distribution, grade and mineralogy, are products of metasomatism. This paper takes a new look at the metamorphism event, with the aim of understanding the effects on the mineral system by providing constraints on the current distribution, chemistry and mineralogy of the deposit, consistent with its evolution constrained by geochronology, isotopes, and geological observations. A coherent and rational argument for the hypothesis is developed using reinterpretation of several sections, 3D geometry of units and re-evaluation of existing data.

A metasomatic origin for many features of Broken Hill is discussed in the context of evidence regarding the metamorphic history, and distribution, mineralogy, grade and chemistry of the ore and alteration. The hypothesis is developed in context of the metasomatic event, using the 5 questions developed and applied to the Century deposit (Ord et al., 2002); viz. (i) What is the structural-lithological architecture and size of the total mineral system? (ii) What was the P-T and geodynamic history? (iii) What was the nature of the fluid reservoirs in the system? (iv) What were the physical and chemical characteristics of the fluids and where were the fluid reservoirs? (v) What were the fluid deposition processes and mechanisms?

## What is the structural-lithological architecture and size of the total mineral system?

<u>Pre-metamorphic Mineralisation</u>

Pb isotopes indicate Broken Hill ore formation age at 1675 Ma (Sun et al, 1996), and the remarkable homogeneity of the Pb isotopes indicates a homogenous ore fluid with little or no subsequent modification (Carr and Sun, 1996; Parr et al., 2003). The genesis and distribution of the original ore system are unclear, with many hypotheses covering all imaginable scenarios from syngenetic to post-metamorphic epigenetic. Several workers indicate the ore was originally deposited in its present disposition of stacked lenses of different mineralogy and chemistry reflecting syngenetic processes (Johnson and Klinger, 1975) or "inhalative" processes (Wright et al., 1993). Metamorphism of the deposit has been viewed as essentially "isochemical" (Stanton, 1976; Scott et al., 1977), but there is a range of views as to how much remobilisation has occurred and the scale of movement of ore minerals. There is considerable debate on whether the ore is largely *in situ* (Webster, 1996) or remobilised and tectonic (Rothery, 2001). Webster (1996) argues that the ore has not moved from its stratigraphic position; however he also argues for metasomatic events and "extensive redistribution of sulphides within 3L [lens]". Several reconstructions of the deposit prior to metamorphism show a series of unfolded, stacked lenses (eg. Plimer, 1979); however recent recognition of high-grade [temperature] shear zones along the line of lode indicate some modification of pre-metamorphic ore geometry is likely. Recognition of these shear zones also implies the water activity during metamorphism is not uniform; some domains between shear zones may be have had little fluid activity (apart from dehydration reactions).

<u>Host Rocks and Ore Lenses</u>

The local mine sequence comprises granitic gneisses, locally taken as a straitgraphic unit marking the top of the Thackaringa Group; Broken Hill Group with psammitic to pelitic metasediments, amphibolites, "Potosi Gneiss", a garnetiferous quartzo-feldspathic gneiss (also Hores Gneiss) shown by Laing et al. (1984) and Laing (1996) to be a volcanic, and lode rocks; then Sundown Group of psammitic to pelitic metasediments.

The stratigraphy hosting the ore consistently dips to the west at about 70º, but is complicated by a probable F1, isoclinal fold nose. This causes a mirror-image of the sequence (Fig. 2), in a similar way to Laing et al's (1978) nappe model for the North mine area, and superposed F2 shear zones and later structures. The stratigraphy is difficult to unravel in the intensely altered area of lode rocks.

Ore lenses form a near-vertical stack (from the top, C-B-A-1-2-3) with each lens having a distinctive mineralogy and average grade (Johnson and Klinger, 1976). The upper lodes (C, B, A, 1 lens) have traditionally been termed the zinc lodes, while the lower 2 and 3 lenses termed lead lodes, and that usage is continued here.

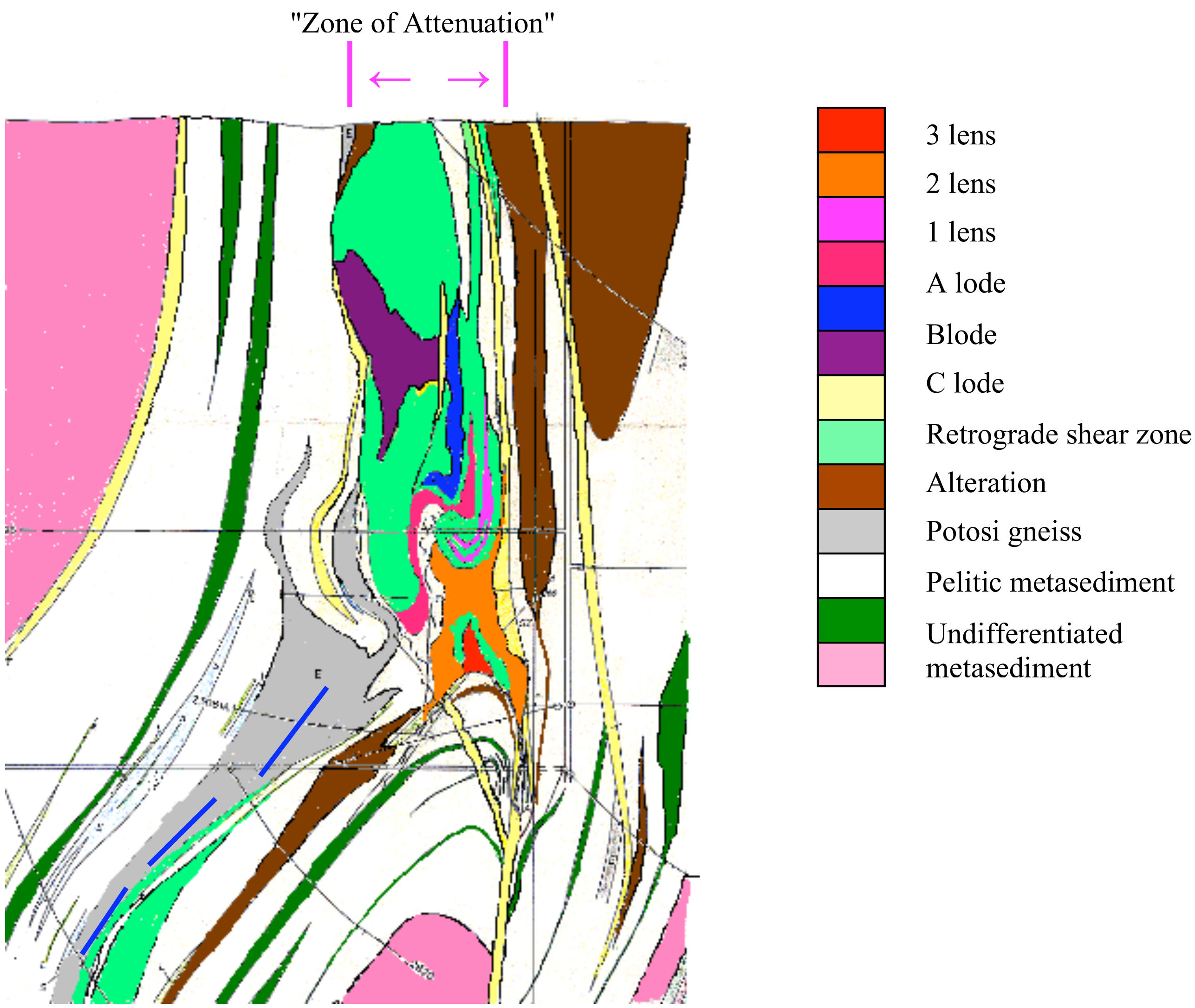


*Fig. 1 Section 30 (looking NE), southern line-of-lode, showing stacked ore lenses in the "Zone of Attenuation". A possible F1 fold axis (blue), is based on symmetry of Broken Hill Group and granite gneisses. Note gross discordance of ore lenses and alteration with the stratigraphy.*

In the south – central part of the deposit (Fig. 1) lodes are in a near-vertical stack within intensely altered lode rocks of "garnet quartzite". The ore lenses are coincident with a unique structural position, recognised by Gustafson et al. (1950) and termed the "Zone of Attenuation". This permissive zone comprises an open fold pair (the Eastern Syncline and Western Anticline; Johnson and Klinger, 1976; also "Main Drag Fold", Rothery, 2001), which often contains the lenses.

Mapping and logging of No. 2 shaft section at the North Mine (Fig. 2) shows several differences to the southern – central lode. There is no area of siliceous alteration in an equivalent position to the zinc lodes; the lead lodes are constrained by an interpreted isoclinal fold close to the Broken Hill Group – Sundown Group contact, also contained within the high-grade shear zone. The 3 lens garnet "sandstone" envelope is crosscutting and post-dating high-grade fabrics, within a broader “lode” zone which is largely an altered sillimanite-quartz-garnet-sericite rock. The zinc lodes appear not to be developed while the lead lodes occur within an isoclinal fold at the Broken Hill-Sundown Group contact. The lead lodes are discordant (Hobbs, 1966), parallel sulphide-rich rods with garnet rims occur within metasediments typical of Sundown Group (i.e. interbedded psammopelite with epidosites [calc-silicate ellipsoids]).

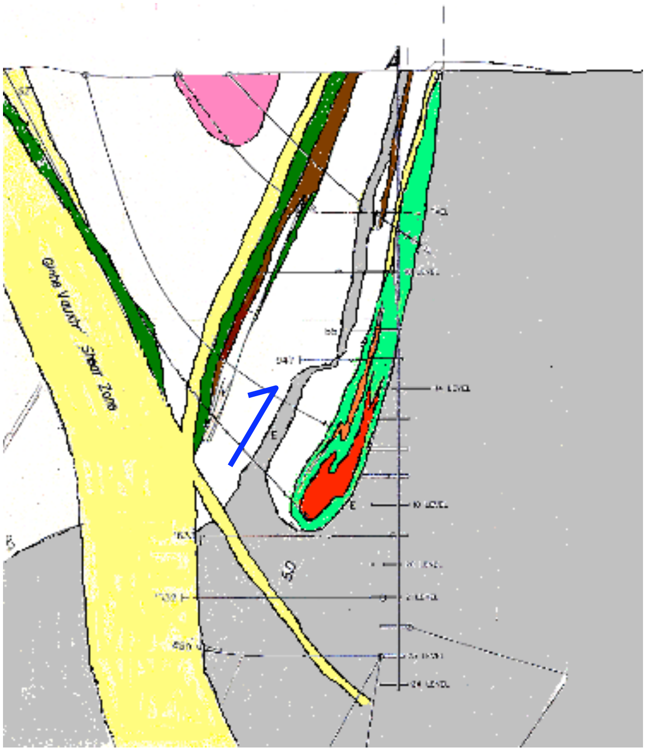

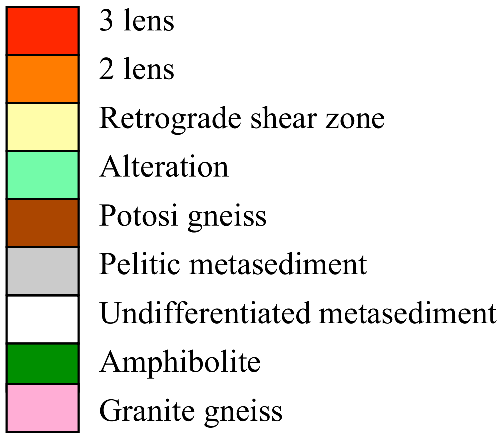


*Fig. 2 Cross section of the No 2 Shaft (North Mine). Blue arrow shows sense of shear for high grade shear zone.*

A deposit long section (Fig. 3) shows plunges that that the ore lenses are consistent with the strong sillimanite lineation and parallel fold plunges in the central and southern parts of the lode. However, the lead lodes have an anomalous steep north plunge at the North Mine, and have been shown to be discordant (Hobbs, 1966). It has been assumed that the zinc lodes also plunge north, parallel to the lead lodes, at this point, but are poorly developed. Mineralisation on the northern leases (Potosi, Silver Peak, Flying Doctor) comprises shallowly plunging lenses complicated by retrograde shearing.

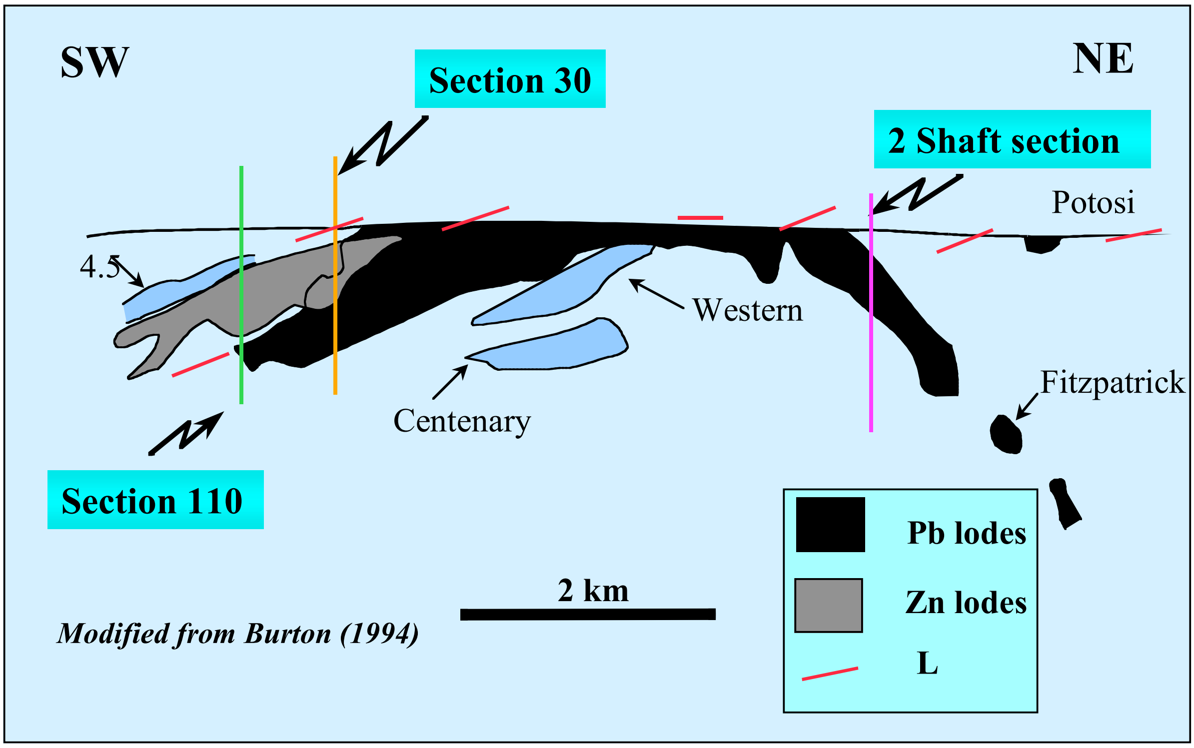


*Fig. 3 Long section of the Broken Hill deposit (after Burton, 1994). L is probable D2 lineation of sillimanite and fold plunges.*

The overall conformable nature of the ore lenses (Johnson and Klinger, 1975) is not supported by the complexity of the structure along the line of lode. Isoclinal F1 folds are overprinted by high-grade shear zones, whereas the ore lens geometry is relatively simple fold pair trending obliquely to the folded stratigraphy (Fig 1).

<u>Ore Zonation and chemistry</u>

Broken Hill is well known the zonation of ore/gangue mineralogy and metal grades, as shown by Johnson & Klinger (1975) and summarised below:

- C lode: low grade (av 4 % Zn, 2% Pb) disseminated and stringery mineralisation in quartz-gahnite-garnet (-feldspar) lode rock.
- B lode: Zn-rich mineralisation, high Zn:Pb ratio; extensive volumes of low grade ore in gangue of quartz, feldspar, garnet, apatite, gahnite, damourite, rhodonite, calcite, manganhedenbergite
- A lode: Gangue rhodonite, manganhedenbergite, quartz, calcite, garnet
- 1 lens: Gangue quartz, calcite, wollastonite, bustamite

- 2 lens:  Calcite, rhodonite, bustamite, manganhedenbergite, roepperite, quartz, garnet, fluorite, apatite
- 3 lens: Rhodonite, fluorite, quartz, garnet.  Highest grades and lowest Zn:Pb ratios.
- Droppers: these are masses of high grade sphalerite-galena with thin garnet "sandstone" alteration rims.  Host rock to the droppers is typically retrograde sericite schist.

Ore lens chemistry (from Johnson and Klinger, 1976) was tested for Rank Correlation with lens order B-A-1-2-3, to assess the validity of changes in chemistry within the sequence of stacked lenses.  There are strong correlations between lens order (B, A, 1, 2, 3) and increasing Ag,  Sb, Pb and F; negative correlation of lens order with Bi; correlation of Pb and F with Ag and Sb (all with each other); correlation of Cd with Zn; and negative correlations of F, Pb and Sb with Bi.  These correlations are interesting in the context of models of ore formation, as a model must explain these effects if the model is to be supported.

Alteration

There are several styles of alteration and degrees of alteration intensity, in the district known as "lode" including garnetites of several variants between garnet quartzite and garnet sandstone, also quartz gahnite, and lode pegmatite.  The siliceous halo (locally "garnet quartzite" is mainly silica with minor garnet and gahnite) and occurs around zinc lodes and is depleted Na, Sr Ca and Mg content (Plimer, 1979) and comprises massive siliceous rock with scattered garnets, dated at 1589 Ma (Ehlers et al, 1996) indicating a post-peak metamorphic age.

Gustafson et al (1950) describe gradations between garnet quartzite and garnet "sandstone" envelopes.   These garnetites are clearly post- high-grade fabrics yet surround massive sulphide lenses with high grade mineralogy.  Hodgson (1975) showed these are not true sandstones and are associated with the high grade metasomatic event, while some garnetites have been shown convincingly to be related to the retrograde event by Jones (1968).

Other typical lode rocks that are regarded here as part of the alteration include the classic quartz-gahnite, typically of bluish quartz and gahnite ± minor feldspar, sulphides and garnet, and lode pegmatite is an unusual rock comprising blue quartz, green to grey, lead-rich K feldspar ± sulphides and garnet. Biotite and K feldspar are locally abundant in the ore environment and may represent more distal (to ore) potassic styles of alteration. Examples include biotite garnetites and biotite-sillimanite-(magnetite) schists.

Intense alteration along the line-of-lode occurs within a volume of approx 10km length, 1 km vertically and 0.2 km across strike, giving a volume of approx 2 $km^3$, although this is within a larger volume of less intense alteration.

**What was the P-T and geodynamic history?**

Gibson and Nutman (2004) propose D1 extension with a detachment at the Broken Hill Group - Sundown Group boundary at 1720-1670 Ma, with associated intrusion of amphibolite and granite gneisses, and metamorphism. Their D1 age encompasses deposition of the Thackaringa Group and Broken Hill Group was between about 1705 and 1680 Ma (Page et al., 2000; Page et al., in prep.). Early shear zones such as the detachment and a high-grade magnetite-sillimanite shear zone in the Broken Hill Synform, described by Noble, 2000, are folded by F2.

The geometry of D1 structures are still enigmatic. Laing et al. (1978) proposed nappe model for D1 along the line-of-lode, however this was disputed by Rothery (2001) due to multiple high-grade shear zones. Nevertheless, symmetry on the line-of-lode using pseudo-stratigraphic markers amphibolite and granite gneisses implies F1 fold axis may be present, albeit considerably disrupted.

Structures associated with the earlier events are controversial. D1 structures are still enigmatic and poorly defined regionally. Laing et al., 1978, developed a nappe model in the mine area, which was extended to the district (Laing, 1996). However along the line-of-lode high-grade (temperature) shear zones were recognised by White et al., 1995, and account for some of the complexity here.

Following the D1 event and crustal thinning, the D2 event, constrained at 1600-1590Ma (Page and Laing, 1992), was probably associated with crustal thickening and peak metamorphism. Upright F2 folds on the line-of-lode have upright, NE trending axial planes and shallow south-west plunges (0 to 25º S) and sillimanite lineation; ore is parallel to this fabric over much of the deposit, however 2 and 3 lenses at the North Mine do not fit this paradigm and are on an oblique trend to this.

Prograde metamorphic conditions for Broken Hill are estimated at 730ºC to 830ºC and 4-7.5 kbar (from THERMOCALC; Mangion, 1998), which encompasses the range estimated by Phillips (1980). Timing of metamorphism is 1600-1590 Ma, significantly after deposition of the Willyama Supergroup generally bracketed in the 1700-1640 Ma range. There is as yet no direct evidence of metamorphism event prior to 1600 Ma but this cannot be ruled out. Mineral assemblages in the deposit are likely (re)crystallise during cooling of this event at <500°C, estimated to have occurred at 1570 Ma (Stevens, 1986).

D3 structures probably encompass a range of events from post-prograde to Delamerian. "Retrograde" shear zones (actually upper greenschist to lower amphibolite grade) have distinctive sericite-chlorite ± garnet, staurolite mineralogy and truncate ore in most places. At the North mine, ore lenses are terminated by and are smeared through Globe Vauxhall Shear Zone, emerge into the Fitzpatrick ore zone then are sheared into Western Shear Zone. Similarly, the lode horizon is clearly offset by DeBavay Shear. Ore lenses in retrograde shear zones are clearly sheared and contain distinctive remobilised features including durchbewegung texture (Marshall and Gilligan, 1989) and garnetite rims (eg. Jones, 1968).

**What was the nature of the fluid reservoirs in the system?**

The metasomatic fluid reservoir must have been close the present ore deposit to the for account for the processes proposed to form and control the distribution of ore and alteration. The most likely reservoir is that generated by dissolution of the initial (pre-metamorphic) mineral assemblages, which by analogy with other Preoterozoic base metal deposits (such as Century; Broadbent et al., 1998) and Pb-Zn-Fe sulphides and Mn-Fe-Ca carbonates.

**What were the physical and chemical characteristics of the fluids?**

*Metasomatism Fluids*

Evidence including high temperature fluid inclusions (Prendergast, 1996), large scale metasomatism of alteration assemblages (Evans, 2002), extensive hydrous retrogression at high T (764+/-27°C) at Round Hill (Swapp and Frost, 2003) and zoning of ore lenses can be explained by fluid activity during waning metamorphism.

Some constraints on these fluids are:

1. The solute: assumed to be a hot metamorphic fluid derived by dehydration reactions. Critical parameters are: T=750°C; $H_2O$ dominated with high $CO_2$, also $N_2$ and $CH_4$. NaCl and KCl may be present in such fluids (Markl and Bucher, 1998).
2. The resultant metal-bearing fluid, derived from reaction of the metamorphic fluid with the primary ore system, and from which the most of the ore was deposited. Evidence for the chemistry of this fluid is that it contained percent levels of Mn, Pb and Zn; high $SiO_2$ is indicated by abundant blue quartz in the lode horizon rocks.

The first question is related to dissolution of ore, and the alternative here is whether the ore is recrystallised *in situ* by non-aqueous recrystallisation, or dissolved by a fluid derived from dehydration reactions that were produced during the prograde event. It seems reasonable to assume some reaction with the ore system, due to existing architecture especially faults and enhanced permeability that allowed the orebody to form there. An undersaturated (with respect to metals), hot fluid would cause extensive dissolution or ore minerals. Indirect evidence for this dissolution and subsequent deposition as new mineral assemblage is the high temperature, skarn-like mineralogy.

At granulite grade, the presence of any aqueous fluid will trigger partial melting, and this is exactly what is seen in close proximity to ore - abundant pegmatites of several generations. In fact some pegmatites are known to separate some of the ore lenses - the "separation pegmatite" between A and B lodes (Johnson and Klinger, 1976) and the famous lode pegmatites. Another consequence of a hot aqueous fluid in such an environment would be the interaction of this fluid with partial melt fluid, generating the famous "lode pegmatite" with its amazonite - blue quartz - sulphide mineralogy.

**Melting of Sulphides**

The hypothesis of Mavrogenes et al. (2001) and Frost et al. (2002) that the Broken Hill sulphide deposits had melted during prograde metamorphism deserves serious consideration. There is some textural evidence of sulphide melts forming at Broken Hill; graphic intergrowths are recorded in some instances mainly in mineral assemblages with high Ag and sulphosalts (Plimer, pers. comm. 2003) which would be expected to have lower eutectic than the bulk of the deposit. A sulphide melt fluid is likely at least locally (eg. Sparks, 2003), however, appears a relatively uncommon phenomena.

Progressive freezing of the sulphide melt would occur during waning metamorphism if the system was anhydrous. Progressive melting of the ore from 500ºC to 795ºC (the quaternary eutectic for the PbS-ZnS-$Ag_2S$ system at 5 kbar) would form sulphide melts within the established metamorphic conditions. A high-temperature sulphide melt would be expected to comprise minerals with lowest melt temperature (eg. galena-tetrehedrite). If such a melt was formed, "restite" would comprise less soluble components such as silica, sphalerite, chalcopyrite and pyrrhotite, as represented in the zinc lodes.

**What were the fluid deposition processes and mechanisms?**

Several processes are implicated in the formation of ore lenses with different lens compositions. The metasomatic event appears a complex system with interplay of variables including timing, temperature, fluids, wall rocks, deformation and pressure.

*Metasomatic reaction during the high-grade event*

A possible and logical explanation for the origin of the siliceous -(gahnite-garnet) alteration lies in the presence of a metal-rich fluid during the high grade metamorphism. Such a fluid would cause generation of melts, manifest as abundant pegmatites. These are demonstrably of several generations in the near-mine environment. If pegmatite is present while the metal-rich fluid is maintained at high temperatures, the reaction produces significant molal amounts of silica, with gahnite, and releases potassium which is also known to be enriched in the Broken Hill alteration system:

$Zn^{++} + 2KAlSi_3O_8 \rightarrow 6SiO_2 + ZnAl_2O_4 + 2K^+$

Zn + k-feldspar → silica + gahnite + potassium

The large amounts of silica formed by this reaction may also explain many features of the gangue assemblages by allowing reaction of original ore components (Ca, Mn, Fe) with silica to form silicates over a range of temperatures consistent with a paragenesis of hot, anhydrous to hydrous and sulphide as cooling progresses. Lode pegmatite, with grey to green lead-rich feldspar and blue quartz occurs in close spatial relationship to ore, within the broader siliceous alteration to the deposit. It is suggested these form by interaction of Pb in the metal-bearing hot fluid with the pegmatite melt.

Thus the hypothesis explains the abundance of several generations of pegmatite, formation of quartz gahnites and siliceous alteration.

*Synchronous mineral deposition and high grade shearing*

The hypothesis is that, during waning of the prograde metamorphic event, cooling of the metal-bearing fluid with fractionation and sinking of a progressively enriched and dense fluid occurred. This was during the D2 structural event, with shearing and boudinage promoting formation of dilational zones. Wall-rock reaction of sulphide-rich fluids produced garnetites.

There is a clear relationship of ore with Main Drag Fold within the "Zone of Attenuation" (Gustafson, 1950); this is given late D1 to D2 timing by Rothery (2001). The resultant ore geometry is akin to saddle reefs, with good down-plunge continuity and aspect ratios (length:width:height) of ore lenses of 1,000:100:10. Boudinage has significant influence on the line of lode (eg. Findlay, 1994; Rothery, 2001), and focus of ore in boudin necks and fabrics along the lineation direction are likely at least in the central and southern parts of the deposit. As ore lenses are contained within this structure, the proposed mechanism is akin to vein formation by crack-seal mechanism, with pressure release causing fluid inflow from the surrounding reservoir. This explains many of the "remobilised" vein and breccia textures of the ore (Hodgson, 1975a).

As noted by Stanton (1983) the Broken Hill ore assemblage is skarn-like. There appears a distinct trend in ore/gangue from pre-ore anhydrous (pyroxene/pyroxenoid) to hydrous (amphibole, garnet) and sulphide, as is the case with Cannington (Bodon, 1996). However, synchronous deformation along the line-of-lode is now known with high-grade shear zones, directly related to the timing of growth of fine-grained garnets in altered garnet-sillimanite-quartz schists adjacent to the ore lenses.

To explain the chemical and mineralogical trends in the ore, fractionation of a dense, metal rich fluid is proposed. Two concurrent processes are shearing on the high grade, line-of-lode shear, with progressive fractionation and sinking of this progressively more Pb-rich (thus heavier) liquid. The ore lenses are hosted by open folds developed during the prograde event (Rothery, 2000) and are suggested to have formed during gaping of these folds during shearing.

Hobbs' (1966) recognition the "the orebody [2 and 3 lenses at North Mine] was not parallel to the foliation prior to the first recognisable structural and metamorphic events in the area" still allows that these deposits were originally disconformable and metamorphosed *in situ*, or that the ores were emplaced disconformably during the metamorphic (metasomatic) event. This second possibility has some support in the post-peak metamorphic garnetite rim around these lenses, and their presence in the high-grade shear zone. It is interpreted that, at North Mine 2 and 3 lenses are large discordant highly remobilised, or they are at the base of a vertically attenuated sequence (Fig. 2), or are aligned within a dilational site formed during boudinage; however, the localisation of these ore lenses remains poorly understood.

Garnet "sandstone" comprising thin (1-3 m) envelopes of fine-grained, Mn garnetite completely enveloping rod-like massive sulphide lodes. The mineralogy and origin of this style appears quite different from the "garnet quartzite". Hodgson (1975, a,b) and Gregory et al., 2003, provide evidence of a high-grade metasomatic Ca-Mn selvedge, formed through the reaction of a sulphide-rich fluid with the wall rocks. These Mn-Ca-Fe garnets appear chemically quite different to the metasedimentary, andradite-rich garnets that may be incorporated as relicts in the earlier siliceous overprint, but there is probably a continuum between the two endmember garnet types resulting from a continually evolving metasomatic process.

**Zone refining**

A process of metasomatically "refining" or upgrading of the Broken Hill ore system is proposed here for the first time, and envisages dissolution of ore minerals by a metamorphic fluid, in order of increasing solubility (Ag>Pb>Zn) and re-deposition in reverse order at structural sites during waning metamorphism.

Zone refining is a process previously documented in VHMS deposits whereby metals were deposited, then resolved and re-deposited by an increasing hydrothermal system (Eldridge et al., 1983). We consider a similar process for re-constituting much of the metallic component of Broken Hill during the prograde metasomatic event. In the low grade halo of pre-metamorphic ore, Ag, Pb and Zn (in that order) are scavenged by metasomatic fluids in order of solubility, and deposited in reverse order.

Thus the metasomatic system becomes relatively increased in Pb and Ag. This gives preferential upgrading of Pb and Ag (the BHT signature metals!), while less soluble minerals remain in upper, more Zn-rich lenses within massive siliceous alteration zone. Differential sinking (due to high density) of a metal and sulphide-rich fluid gives rise a fractionated system with progressive concentration in Ag, Pb, Sb, F, Mn and Zn, as well as the ratio Ag:Pb:Zn. Hypothetical examples of the effect of zone refining on an ore system are given in Fig.4

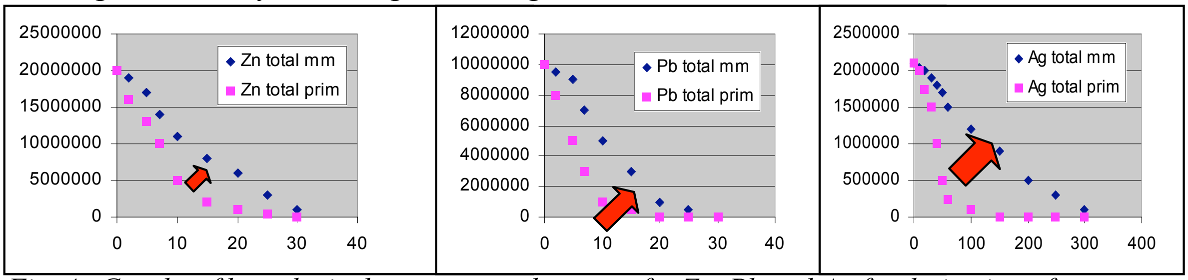


*Fig. 4. Graphs of hypothetical tonnage-grade curves for Zn, Pb and Ag for derivation of current ore grades (blue diamonds) from a pre-metamorphic ore (purple squares). X axis is total contained metal (tonnes for Zn, Pb; g/100 for Ag) Y axis is cutoff grade. Increasing solubility of Zn →Pb →Ag gives rise to an increasingly high grade component. Arrows shows the approximate relative extent of upgrading.*

An efficient leaching process would have the effect of upgrading the deposit in the order of solubility, and taking previously low grade mineralisation in any low grade envelope and forming high-grade sulphides preferentially enriched in Ag and Pb, but also Zn. This process may explain the "unusual" metal ratios in the enigmatic class of "Broken Hill-type" deposits.

## Implications

The metasomatic overprint of the ore system is believed to generated many of the characteristics of Broken Hill and, by analogy, other Broken Hill-type deposits. Pre-existing mineralisation and alteration was therefore unlike that existing now.

Comparison with Century, as a nearly pristine example of a sediment-hosted massive sulphide deposit, shows some common features in the host rock succession. The Broken Hill host rocks comprise psammitic to pelitic, often graded and interpreted as turbiditic sandstones (Laing et al., 1978), while at Century turbiditic sandstones form a significant component of the Lawn Hill Formation (Andrews, 1998). The host at Century is a shale unit (unit H4 of Lawn Hill Formation), while at

Broken Hill pelitic units (locally the "4.6 pelite") occurs closely tied to the zinc lode position.

For Broken Hill, the implications of this hypothesis are that the ore is indeed structurally controlled, within the "Zone of Attenuation". High grade shear zones are now known to be at least in part coincident with this zone. The geometry of the ores, with high linearity and largely confined with the "Main Drag Fold" and similar structural traps.

BHT deposits with alteration and ore features like Broken Hill may have a similar origin. Local controls on the metasomatic event involving ore solution and re-deposition, will be critical in controlling ore lens shape, mineralogy and grade. These controls are likely to be both structural and related to fluid density and reactions with fluids and wall rocks. The original (pre-metamorphic) ore system is likely to be difficult to decipher through a major metasomatic event

Other well-known base metal styles have alteration patterns unlike that at Broken Hill. Sediment-hosted deposits have subtle carbonate alteration (eg. Century, Broadbent et al., 1998); carbonate-hosted deposits often have different carbonate chemistry near ore, while VHMS deposits typically have zoned footwall alteration marked by Mg enrichment and Na depletion.

**Acknowledgements**

The author would like to thank Bob Haydon for many discussions on Broken Hill, inspiration from Bruce Hobbs to complete this work, and acknowledge ideas from Roger Powell and Pat Williams that contribute to the hypothesis. The work behind this paper results from the C1 Curamona project within the *pmd**CRC.

**References**

Andrews, S., 1998. Stratigraphy and depositional setting of the upper McNamara Group, Lawn Hills region, Northwest Queensland; Econ. Geol., 93, 1132-1152.

Bodon, S. B., 1996. Genetic implications of the paragenesis and rare-earth element geochemistry at the Cannington Ag-Pb-Zn deposit, Mt Isa Inlier, northwest Queensland; *in* Ponzgratz, J and Davidson, G, eds: New Developments in Broken Hill Type Deposits; CODES Spec Pub 1; 133-144; University of Tasmania.

Broadbent, G. C., Myers, R. E. and Wright, J. V., 1998. Geology and origin of shale-hosted Zn-Pb-Ag mineralization at the Century deposit, northwest Queensland, Australia; Econ. Geol., 93, 1264-1294.

Carr G.R. and Sun S.-S., 1996, Lead isotope models applied to Broken Hill style terrains: syngenetic vs epigenetic metallogenesis; i*n:* Pongratz, J. and Davidson, G., (editors): *New Developments in Broken Hill Type Deposits*. CODES Special Publication 1, 77-86.

Eldridge, C. S., Barton, P. B. Jnr., and Ohmoto, H., 1983. Mineral Textures and Their Bearing on Formation of the Kuroko Orebodies; *in* H. Ohmoto and B. J. Skinner (eds.) The Kuroko and Related Volcanogenic Massive Sulphide Deposits; Econ. Geol. Mon. 5, 241-281.

Evans D., 2002, Nature and Origin of the Lithochemical Halo across Section 110 of the Broken Hill Zn-Pb-Ag Deposit, BSc (Hons) Thesis, LaTrobe Univ (unpub.).

Findlay, D., 1994. Boudinage, a reinterpretation of the structural control on the mineralisation at Broken Hill; Aust. Jour. Earth Sci., 41, 387-390.

Frost, B. R., Mavrogenes, J. A., and Tomkins, A. G., 2002. Partial melting of sulfide ore deposits during medium- and high-grade metamorphism; Canadian Mineralogist, 40, 1-18.

Gibson, G. M. and Nutman, A. P., 2004. Detachment faulting and bimodal magmatism in the Palaeoproterozoic Willyama Supergroup, south-central Australia: keys to recognition of a multiply deformed Precambrain metamorphic core complex; Jour. Geol. Soc. Lond., 161, 55-66.

Giles, D. and Nutman, A. P., 2002. SHRIMP U-Pb monazite dating of 1600-1585 Ma amphibolite facies metamorphism in the south-eastern Mt Isa Block, Australia; Aust. Jour. Earth Sci., 49, 455-466.

Gregory, R. W., Swapp, S. M., Frost, B. . and Mavrogenes, J. A., 2003. Evidence for High-T Mn- and Ca-Metasomatism in the Broken Hill Ore Package; Abstracts, 2003 Seattle Annul Meeting, Geol. Soc. America.

Gustafson, J. K., Burrell, H. C. and Garretty, M. D., 1950. Geology of the Broken Hill Ore Deposit, Broken Hill, N.S.W., Australia; Bull Geol Soc Am, 61, 1369-1438.

Hobbs B. E., 1966. The structural environment of the northern part of the Broken Hill orebody; Jour Geol. Soc. Aust., 13, 315-338.

Hodgson, C. J., 1975a. The Geology and Geological Development of the Broken Hill Lode, in the New Broken Hill Consolidated Mine Australia, Part II: Mineralogy; Jour Geol. Soc. Aust., 22 (1), 33-50.

Hodgson, C. J., 1975b. The Geology and Geological Development of the Broken Hill Lode, in the New Broken Hill Consolidated Mine Australia, Part III: Petrology and Petrogenesis; Jour Geol. Soc. Aust., 22 (2), 195-213.

Johnson, I. R. and Klinger, G. D., 1976. The Broken Hill ore deposit and its environment; *in* Economic Geology of Australia and Papua New Guinea, 1. Metals; Aus. I. M. M. Mon. 5, 476-491.

Jones, T. R., 1968. Garnet Sandstone and Garnet Rims at Orebody Contacts, Broken Hill; in Broken Hill Mines – 1968 (ed M Radmanovich and J T Woodcock), Aus. I. M. M. Mon. 3, 171-178.

Laing, W. P., Marjoribanks, R. W. and Rutland, R. W. R., 1978. Structure of the Broken Hill Mine Area and its Significance for the Genesis of the Orebodies; Econ. Geol., 73, 1112-1136.

Laing, W. P., Sun, S. S. and Nesbitt, R. W., 1984. Acid volcanic precursor to "Potosi" gneiss at Broken Hill and its implications for ore genesis; 7th Australian Geological Convention, Geol. Soc. Aust. Abs 12: 318-321.

Laing, W. P., 1996. Nappe interpretation, palaeogeography and metallogenic synthesis of the Broken Hill – Olary Block; *in* Ponzgratz, J. and Davidson, G., eds: New Developments in Broken Hill Type Deposits; CODES Spec Pub 1; 21-51; University of Tasmania.

Mangion C., 1998, The structural setting of the southern termination of western A lode, Broken Hill, NSW; B.Sc (*Hons)* Thesis, Univ of Melb (unpub.).

Markl, Gregor and Bucher, Kurt, 1998, The presence and composition of fluids in the lower crust as inferred from metamorphic salt in granulites. Nature 391, 781-783.

Marshall, B. and Gilligan, L B., 1989. Durchbewegung Structure, Piercement Cusps, and Piercement Veins in Massive Sulphide Deposits: Formation and Interpretation; Econ. Geol., 84, 2311-2319.

Mavrogenes, J. A., MacIntosh, I. W. and Ellis, D. J., 2001. Partial melting of the Broken Hill Galena-Sphalerite Ore: Experimental Studies in the System PbS-FeS-ZnS-($Ag_2S$); Econ. Geol., 96, 205-210.

Noble, M P, 2000. The Geology of the Broken Hill Synform, N.S.W., Australia; MSc thesis, Monash University (unpub.).

Page, R. W. and Laing, W. P., 1992. Felsic Metavolcanic Rocks Related to the Broken Hill Pb-Zn-Ag Orebody, Australia: Geology, Depositional Age, and Timing of High-Grade Metamorphism; Econ. Geol., 87, 2138-2168.

Page, R. W., Stevens, B. P. J., Gibson, G. M. and Conor, C. H. H., 2000. Geochronology of Willyama Supergroup rocks between Olary and Broken Hill, and comparison to northern Australia; *in* Peljo M. (compiler) Broken Hill Exploration Initiative 2000, conference abstracts; AGSO Record 2000/10, 111p.

Page, R. W., Stevens, B. P. J., and Gibson, G. M., in prep. Geochronology of the sequence hosting the Broken Hill Pb-Zn-Ag orebody.

Parr, J.M., Stevens, B.P.J. and Carr, G.R., 2003, Timing of multiple hydrothermal events in the Broken Hill terrain – evidence from lead isotopes. *in* Peljo M. (compiler), Broken Hill Exploration Initiative 2000, conference abstracts; AGSO Record 2003/13, 126-129.

Phillips, G. N., 1980. Water activity changes across an amphibolite-granulite facies transition, Broken Hill, Australia; Contrib. Mineral. Petrol., 75, 377-386.

Pidgeon, R. T., 1967. A Rubidium-Strontium Geochronological Study of the Willyama Complex, Broken Hill Australia. Journal of Petrology, 8 (2), 283-324.

Plimer, I. R., 1979. Sulphide rock zonation and hydrothermal alteration at Broken Hill, Australia; Trans I. M. M. (Sect B), 161-176.

Plimer, I. R., 1985. Broken Hill Pb-Zn-Ag deposit – a product of mantle metasomatism; Mineral Deposita, 20, 147-153.

Prendergast K., 1996, The paragenesis of Western A lode, Broken Hill , New South Wales, B. Sc. (Hons) Thesis, James Cook Univ. N. Qld. (unpub.).

Scott, S.D., Both, R.A. and Kissin, S.A., 1977. Sulfide Petrology of the Broken Hill Region, New South Wales; Econ. Geol., 72, 1410-1425.

Sparks, H. A., 2003. Application of LA-ICP-MS to Sulphide Melt Inclusion Analysis: Example from Broken Hill; Abstracts, 2003 Seattle Annul Meeting, Geol. Soc. America.

Stanton, R. L., 1976. Petrochemical studies of the ore environment at Broken Hill, New South Wales, parts 1, 2, 3 and 4; Trans. Inst. Min. Metall., (Sect. B), 85, B33-46, B118-131, B132-141, B221-233.

Stanton, R. L., 1983. Stratiform ores and Metamorphic Processes - some thughts arising from Broken Hill; Proc. Aus. I. M. M. Conference, Broken Hill.

Stevens, B. P. J., 1986. Post-depositional history of the Willyama Supergroup in the Broken Hill Block, N.S.W., Aust. Jour. Earth Sci., 33, 73-98.

Sun S.-S., Carr, G.R. and Page, R.W., 1996, A continued effort to improve lead-isotope model ages. Australian Geological Survey Organisation Research Newsletter, 24, 19-20.

Swapp, S. M. and Frost, B. R., 2003. Evidence for high-pressure metamorphism in the granulites of the Broken Hill area; *in* Peljo M. (compiler) Broken Hill Exploration Initiative 2003, conference abstracts; AGSO Record 2003/13.

Webster, A. E., 1996. A detailed description of the Broken Hill deposit – lessons from the ore fabrics; *in* Ponzgratz, J and Davidson, G, eds: New Developments in Broken Hill Type Deposits; CODES Spec Pub 1; 95-103; University of Tasmania.

White, S. H., Rothery, E, Lips, A. L. W. and Barclay, T. J. R., 1995. Broken Hill area, Australia, as a Proterozoic fold and thrust belt: implications for the Broken Hill base-metal deposit; Trans I. M. M. (Sect. B), 104; B1-B17.

Wright, J.V., Haydon, R.C. and McConachy, G.W., 1993. Sedimentary analysis and implications for Pb-Zn mineralisation at Broken Hill, Australia; *Geology*, 15 (7) 598-602.

# Appendices (on accompanying CD)

1. New Pb isotope analyses from the Curamona Terrain

    - Parr and Carr Analyses.xls

2. Collation of existing data on previously analysed samples from the Curamona terrain

    - Parr & Carr old sample information.xls

3. High-temperature metamorphism in poly-deformed orogens: A case study of the Proterozoic Broken Hill Block, Australia - Caroline Forbes, PhD Thesis, Monash University

    - Forbes Thesis.zip

4. Nature and origin of the lithogeochemical halo across section 110 of the Broken Hill Zn-Pb-Ag deposit - Darin Evans, BSc (Hons) thesis, La Trobe University

    - Darin Evans thesis BKHSect110.pdf
    - Darin Evans thesis Sect110Final.pdf
    - Darin Evans thesisFinalCopy.doc

5. Geology of the B Lode, A Lode and 1 Lens on CML7, Broken Hill, N.S.W. - Richard Tully BSc (Hons) thesis, La Trobe University

    - Richard Tully_thesis.zip